N69-33876
CR-105287

SCIENTIFIC NOTE

ESRO SN-83
February 1968

E-S-R-O
C-E-R-S

THERMAL ANALYSIS OF SMALL CYLINDRICAL AMMONIA EVAPORATORS

by D.J. Gilson
Royal Aircraft Establishment
Farnborough, Hants

ORGANISATION EUROPÉENNE DE RECHERCHES SPATIALES
EUROPEAN SPACE RESEARCH ORGANISATION

SCIENTIFIC NOTE

ESRO SN-83
February 1968

THERMAL ANALYSIS OF SMALL CYLINDRICAL AMMONIA EVAPORATORS

by D.J. Gilson
Royal Aircraft Establishment
Farnborough, Hants

ORGANISATION EUROPÉENNE DE RECHERCHES SPATIALES
EUROPEAN SPACE RESEARCH ORGANISATION
114, avenue de Neuilly, 92 Neuilly-sur-Seine (France)

Technical Report

AE 6706

Thermal Analysis of Small Cylindrical Ammonia Evaporators

By

David J. Gilson

Department of Aerospace Engineering

University of Cincinnati

Cincinnati, Ohio

August 1967

ABSTRACT

An analysis is presented of the steady state thermal behaviour of small tubular evaporators filled with porous thermally conducting material and exchanging heat by conduction with a hypothetical spacecraft mass.

A particular application is examined in quantitative detail and the criteria for the choice of evaporator shape are discussed. A special type of evaporator construction is derived and compared with the simple type.

An experimental correlation with the theory is performed.

Brief consideration is also given to the transient evaporator conditions.

TABLE OF CONTENTS

LIST OF FIGURES

TABLE OF SYMBOLS USED

A	- internal cross-sectional area of evaporator (ft^2)
c_1, c_2 etc	- constants of known value
d	- cylindrical outer diameter of evaporator (ft)
Cp_E	- mean specific heat of materials comprising evaporator cross-section (Btu/lb ^{0}F)
Cp_{sc}	- specific heat of homogeneous spacecreft material (Btu/lb ^{0}F)
Cp_v	- mean specific heat of ammonia vapour over range of boiling temperatures in evaporator (Btu/lb ^{0}F)
ϵ	- emissivity of outer surface of evaporator
h	- enthalpy of ammonia liquid (Btu/lb)
H	- enthalpy of ammonia vapour (Btu/lb)
ΔH_B	- enthalpy rise of ammonia as it passes through the boiling region (Btu/lb)
k_E	- mean thermal conductivity of evaporator cross-section (Btu/ft hr ^{0}F)
k_F	- effective thermal conductivity of nickel sponge material (Btu/ft hr ^{0}F)
k_{sc}	- effective thermal conductivity of spacecreft (Btu/ft hr ^{0}F)
k_w	- thermal conductivity of evaporator wall (Btu/ft hr ^{0}F)
$K_{1,2}$ etc	- arbitrary constants
L	- mean latent heat of evaporation of ammonia over the range of internal pressures in evaporator (Btu/lb)
λ_B	- length of boiling region in evaporator, measured internally (ft)
λ_S	- length of superheat region in evaporator, measured internally (ft)

λ_T	- total internal length of evaporator (ft)
m	- rate of mass flow of ammonia (lb/s)
M	- mass of ammonia vapour (lb)
P	- mean internal pressure in evaporator (lb/in^2)
q	- rate of flow of thermal energy (Btu/hr)
q_B	- heating rate to boiling region (Btu/hr)
q_C	- rate of conductive heat exchange (Btu/hr)
q_O	- thermal energy flow rate due to radial conduction at the circumference per hr ^0F unit length of evaporator (Btu/ft hr ^0F)
q_R	- rate of radiative heat exchange (Btu/hr)
Q	- thermal energy content (Btu)
Q_E	- thermal energy capacity of evaporator with respect to steady state conditions (Btu)
Q_{SC}	- thermal energy capacity of spacecraft with respect to steady state conditions (Btu)
r	- radius (ft)
r_E	- external cylindrical radius of evaporator (ft)
r_{SC}	- radius of idealized homogeneous sphere representing the spacecraft (ft)
r_{SPH}	- radius of idealized spherical package or sphere equivalent to cylindrical evaporator (ft)
R	- gas constant for ammonia (ft lb/lb ^0F)
ρ_E	- mean density of evaporator cross-section (lb_m/ft^3)
ρ_{SC}	- mean density of spacecraft (including structure and payload) (lb_m/ft^3)
ρ_V	- density of ammonia vapour (lb_m/ft^3)
S	- velocity of flow (ft/s)
σ	- Stefan-Boltzmann constant for radiative heat exchange (Btu/ft^2 hr $^0F^4$)
t_G	- thickness of gap between double walls of evaporator (ft)
t_W	- thickness of evaporator wall or walls (ft)
T	- temperature (^0R)
ΔT	- temperature difference between ambient and mean evaporator cross-section temperatures (^0F)
T_{AMB}	- temperature of surroundings (periphery of spacecraft) (^0R)

T_L - temperature of boiling liquid ammonia at mean internal pressure in evaporator (^{0}R)

ΔT_0 - temperature difference between ambient and boiling liquid ammonia (^{0}F)

T_{SC} - temperature at a point in spacecraft (^{0}R)

ΔT_{SC} - temperature difference between ambient and evaporator wall (^{0}F)

T_{ULT} - temperature attained by ammonia vapour at end of superheat region (^{0}R)

T_V - temperature of ammonia vapour, averaged across a cross-section (^{0}R)

ΔT_V - temperature difference between evaporator wall and mean temperature of evaporator cross-section (^{0}F)

T_W - temperature of evaporator wall (^{0}R)

T_{420} - datum temperature for thermal energy content (^{0}R)

τ - time (hr)

θ - time for saturation of thermal capacity of evaporator and spacecraft (seconds)

W_E - weight of evaporator (lb)

x - axial distance along evaporator, measured internally from inlet (ft)

SUBSCRIPTS (also defined above)

AMB - ambient conditions

B - boiling region conditions

E - evaporator conditions

F - nickel sponge conditions

L - boiling liquid ammonia conditions

S - superheat region conditions

SC - spacecraft conditions

SPH - spherical package conditions

V - ammonia vapour conditions

W - evaporator wall conditions

THERMAL ANALYSIS OF SMALL CYLINDRICAL AMMONIA EVAPORATORS

D.J. Gilson
Royal Aircraft Establishment
Farnborough, Hants.

1. INTRODUCTION

A particular type of resistojet thruster system being developed for spacecraft attitude control employs ammonia as the working fluid. The ammonia is stored as a liquid, passed through an evaporator, and admitted as a dry vapour to the thrust chamber where it is heated by an electric element and expanded through a nozzle to provide a thrust of the order of 10^{-3} to 10^{-2} lb.

The evaporator, working between certain pressure limits, must take in liquid or very wet vapour and convert it to superheated vapour. The thermal energy required for the evaporation and heating of the vapour is obtained from the surroundings, in this case the bulk of the spacecraft. Heat transfer is enhanced by the use of a nickel sponge material which fills the chamber, thereby holding the liquid in its interstices and conducting useful heat from the skin of the evaporator.

The nickel sponge material is General Electric foametal supplied by the General Electric Co. of Detroit. The sponge is also available in copper and iron but corrosion prohibits the use of these materials with ammonia. In its low density form the material has a density of about two to five percent compared with solid nickel.

The thermal analysis of a device using this material does not lend itself to conventional convective heat exchanger theory because of the strong influence of conductive heat flow. Accordingly, a simple means of analysis appropriate to such a system is desired.

2. OPERATING CONDITIONS IMPOSED BY THE THRUSTER SYSTEM

Before approaching the analysis of the evaporator it is necessary to consider the basic constraints imposed by the system as a whole and its intended mode of operation. Reference to Fig. 1, which shows the general layout of the thruster system, will clarify the following discussion.

2.1 MASS FLOW RATE

It is obviously a fundamental requirement that the evaporator should successfully vaporize ammonia at the maximum continuous rate of flow demanded. The maximum demand itself need not necessarily be continuous for, in general, the system will operate on an on-off basis, the period of the cycles being a few seconds, say. However, the analysis will assume continuous flow since the thermal time constant of the evaporator will be found to be appreciably longer than the period of these fluctuations.

2.2 CONDITION OF AMMONIA AT INLET TO EVAPORATOR

In the system considered, the ammonia is stored in liquid form, its temperature in general being the ambient temperature of the spacecraft. The corresponding vapour pressure will be several atmospheres ; typically at 70^0F the vapour pressure is 128.8 lb/in^2. It is essential to the working of the evaporator that it should operate at a temperature well below the ambient one and this is achieved by reducing the pressure in the evaporator.

As shown in Fig. 1, a solenoid on-off valve operated by a pressure switch on the evaporator controls the flow into the evaporator from the ammonia reservoir. Typically, the valve might open at 20 lb/in^2 and close when the pressure had risen to 30 lb/in^2. If one can specify a valve orifice sufficiently small, the expansion into the evaporator will not be too violent and throttling at constant enthalpy conditions can be assumed. Some restriction in the inlet line will be needed anyway to allow time for the pressure switch to react and prevent the pressure building above the intended upper limit. Throttling implies that the liquid ammonia will enter the evaporator as a very wet vapour. Any heating from the surroundings or from friction will result in a vapour slightly drier than that predicted theoretically.

2.3 CONDITION OF AMMONIA AT OUTLET FROM EVAPORATOR

Efficient operation of the thruster system requires that the vapour leaving the evaporator should have as high a temperature as possible, i.e. as close as possible to the ambient temperature. Since the boiling point of the liquid in the evaporator will usually be less than 0^{0} F, while the ambient temperature will be much higher, considerable superheating of the ammonia vapour can be effected by appropriate design of the evaporator.

2.4 ACCUMULATION OF LIQUID IN THE EVAPORATOR

It is also a requirement of the thruster system that the accumulation of liquid ammonia in the evaporator at any time should not be allowed to build up excessively. The object of this precaution is to prevent undue sloshing of liquid ammonia to the outlet end of the chamber under the action of external disturbances.

2.5 PLENUM CHAMBER EFFECT

In addition to its more obvious functions, the evaporator is required to act as a vapour reservoir and reduce the frequency of operation of the solenoid valve which controls the flow to it. This type of valve does not readily meet the ultra-high reliability requirements of spacecraft equipment, and severe restrictions on the permitted number of operations may be required.

2.6 AMBIENT TEMPERATURE

Whatever the mode of heat transfer between evaporator and spacecraft, the temperature difference between the two will obviously have a direct effect on the quantity of heat transmitted.

Since the evaporator temperature will basically be controlled by the thruster system parameters, the ambient temperature of the spacecraft will have a direct effect on the quantity of heat transmitted.

However, the designed ambient temperature limits of a spacecraft will normally be dictated by other requirements than those of the thruster system. In designing an evaporator for a certain application, therefore, the lowest ambient temperature anticipated will usually represent the critical design case.

3. CONDITIONS REQUIRED OR ANTICIPATED WITHIN THE EVAPORATOR

In order to carry out a thermal analysis of the evaporator one must idealize the thermal situation by making various approximations and assumptions.

3.1 SHAPE OF EVAPORATOR

The analysis will be confined to cylindrical evaporators of circular cross-section, the fluid flow being in the axial direction, as shown in Fig. 3.

3.2 AXIAL TEMPERATURE DISTRIBUTION

As previously stated, the nickel sponge has two main functions, to hold the liquid ammonia in its interstices and to conduct heat to the centre from the surface of the evaporator. It is clear that temperature gradients will be set up within the evaporator in an axial direction, the inlet end being cold and the outlet end being warm, and to a lesser extent in the radial direction, the centre being cold and the outer skin warm. Fig. 2 (a) shows that a certain length of the evaporator at the inlet end will be cooled to the temperature of boiling liquid ammonia. This length of the chamber will be referred to as the Boiling Region. It will be filled with a mixture of liquid and wet vapour. The remaining length of the evaporator, which will be referred to as the Superheat Region, will have a temperature varying from that of the liquid to nearly ambient and will hopefully contain only superheated vapour. The line dividing these two regions will be called the Liquid Boundary, for want of a better term. In conventional boiler theory it is usual to consider a wet vapour as an intimate mixture of dry vapour and minute liquid droplets in suspension. Due to the high latent heat of vaporization and the poor heat transfer between the droplets and dry vapour, the droplets may persist even when the bulk of the vapour has been considerably superheated. Now the nickel sponge material, although having a density only a few percent of that of nickel, has a small pore size of the order of 0.020 inches forming a close knit mesh. One may therefore expect that any extraneous droplets penetrating the superheat region will collide with the warmer sponge mesh and be evaporated, thus preserving the well-defined boundary between the two regions.

The exact shape of the liquid boundary is not easily predicted and Fig. 2 (b) shows some possible shapes. Because the axis of the evaporator is farthest from the warm surroundings it will obviously tend to be cooler, thus distorting the boundary to one of the paraboloid shapes shown. However, one can expect that the general turbulence associated with the boiling process will minimize this effect by helping to distribute the liquid phase across the cross-section of the chamber so that the boundary will tend more nearly to form a plane surface normal to the axis of the evaporator, as shown.

It should be noted that in the superheat region, the axial temperature gradient will cause conductive transfer of heat from the warm end to the cold end of the region, and one must allow for this in the analysis. One can ignore here the effect of radiative transfer, which will be small compared with conduction in the nickel sponge, and also the effect of axial conduction in the surrounding spacecraft structure. The conductivity of the ammonia vapour will be extremely small and will also be ignored.

3.3 RADIAL TEMPERATURE DISTRIBUTION

The radial variation of temperature is considered in Appendix I and illustrated in Figure 17.

(a) Boiling Region

Fig. 17 (a) shows the expected type of temperature distribution across the evaporator cross-section. Good contact between the liquid ammonia and all parts of the evaporator section will tend to keep the entire cross-section at the temperature of boiling liquid ammonia.

(b) Superheat Region

Fig. 17 (b) shows the expected distribution in the superheat region. Thermal contact and heat transfer between the gaseous ammonia and the evaporator walls are now relatively poor, allowing the centre of the cross-section to adopt a somewhat lower temperature than the walls, as shown.

3.4 HEAT TRANSFER BETWEEN SPONGE AND AMMONIA

The intimate contact between the nickel sponge and the ammonia will tend to reduce the temperature difference between these two components and one can take advantage of this fact by assuming that at any point in the chamber, the sponge and the ammonia fluid have the same temperature. One is saying, in effect, that there is perfect transfer of heat between the two media or that they can be considered in combination as one homogeneous material.

4. STEADY STATE ANALYSIS OF SUPERHEAT REGION OF EVAPORATOR

A general relationship for the variation of the mean axial temperature in this region must now be obtained. This will be achieved by considering the change of mass content and thermal energy content of an axial element of length Δx, during a period of time $\Delta\tau$.

Initially, we will consider a varying cross-sectional area, i.e. A is dependent on x, and a varying internal pressure, i.e. P is dependent on τ. The temperature in this region will, of course, be dependent on both x and τ.

Fig. 3 pictures the arrangement.

4.1 MASS CONTENT OF ELEMENT

At time τ, the mass of ammonia vapour contained in an element is given by

$$M = \left(\rho_v + \frac{\partial\rho_v}{\partial x} \cdot \frac{\Delta x}{2}\right) \left(A + \frac{\partial A}{\partial x} \cdot \frac{\Delta x}{2}\right) \Delta x$$

but $\rho_v = \dfrac{P}{RT_v}$ assuming the vapour obeys the gas laws.

Therefore

$$M = \frac{P \cdot \Delta x \left(A + \frac{\partial A}{\partial x} \cdot \frac{\Delta x}{2}\right)}{R \left(T_v + \frac{\partial T_v}{\partial x} \cdot \frac{\Delta x}{2}\right)}$$

Similarly, at time $\tau + \Delta\tau$ the mass content is given by

$$M + \Delta M = \frac{\left(P + \frac{\partial P}{\partial \tau} \cdot \Delta\tau\right) \Delta x \left(A + \frac{\partial A}{\partial x} \cdot \frac{\Delta x}{2}\right)}{R\left(T_v + \frac{\partial T_v}{\partial x} \cdot \frac{\Delta x}{2} + \frac{\partial T_v}{\partial \tau} \cdot \Delta\tau\right)}$$

Hence, the increase in mass content of an element in time $\Delta\tau$ is given by

$$\Delta M = \frac{\Delta x \left(A + \frac{\partial A}{\partial x} \cdot \frac{\Delta x}{2}\right)}{R} \left[\frac{P + \frac{\partial P}{\partial \tau} \cdot \Delta\tau}{T_v + \frac{\partial T_v}{\partial x} \cdot \frac{\Delta x}{2} + \frac{\partial T_v}{\partial \tau} \cdot \Delta\tau} - \frac{P}{T_v + \frac{\partial T_v}{\partial x} \cdot \frac{\Delta x}{2}}\right]$$

which reduces to

$$\Delta M = \frac{A}{R} \cdot \Delta x \cdot \Delta\tau \cdot \frac{\partial}{\partial \tau}\left(\frac{P}{T_v}\right) \tag{1}$$

as $\Delta\tau$ and $\Delta x \longrightarrow 0$

Also, at time τ, the rate of mass flow into an element is given by

$$m_{IN} = \rho_v \cdot A \cdot s = \frac{P \cdot A \cdot s}{R \cdot T_v}$$

and the mass flow into an element in time $\Delta\tau$ is given by

$$M_{IN} = \frac{A}{R}\left[\frac{P \cdot s}{T_v} + \frac{\partial}{\partial \tau}\left(\frac{P \cdot s}{T_v}\right) \cdot \frac{\Delta\tau}{2}\right] \cdot \Delta\tau$$

Similarly, the mass flow out of an element in time $\Delta\tau$ is given by

$$M_{OUT} = \frac{\left(A + \frac{\partial A}{\partial x}\Delta x\right)}{R}\left\{\left(P + \frac{\partial P}{\partial \tau} \cdot \frac{\Delta\tau}{2}\right) \cdot \left[\frac{s}{T_v} + \frac{\partial}{\partial \tau}\left(\frac{s}{T_v}\right) \cdot \frac{\Delta\tau}{2} + \frac{\partial}{\partial x}\left(\frac{s}{T_v}\right) \cdot \Delta x\right]\right\} \cdot \Delta\tau$$

Hence, the increase in the mass content of an element in time $\Delta\tau$ is given by

$$M_{IN} - M_{OUT} = \frac{\Delta\tau}{R}\left\{A\left[\frac{P \cdot s}{T_v} + \frac{\partial}{\partial\tau}\left(\frac{P \cdot s}{T_v}\right) \cdot \frac{\Delta\tau}{2}\right]\right.$$

$$\left. - \left(P + \frac{\partial P}{\partial\tau} \cdot \frac{\Delta\tau}{2}\right)\left(A + \frac{\partial A}{\partial x} \cdot \Delta x\right)\left[\frac{s}{T_v} + \frac{\partial}{\partial\tau}\left(\frac{s}{T_v}\right) \cdot \frac{\Delta\tau}{2} + \frac{\partial}{\partial x}\left(\frac{s}{T_v}\right) \cdot \Delta x\right]\right\}$$

which reduces to

$$M_{IN} - M_{OUT} = -\frac{P}{R} \cdot \Delta x \cdot \Delta\tau \cdot \frac{\partial}{\partial x}\left(\frac{A \cdot s}{T_v}\right) \qquad (2)$$

as $\Delta\tau$ and $\Delta x \longrightarrow 0$

The increases in mass obtained by the two approaches must be equal, so equating (1) and (2)

$$A \cdot \frac{\partial}{\partial\tau}\left(\frac{P}{T_v}\right) = -P \cdot \frac{\partial}{\partial x}\left(\frac{A \cdot s}{T_v}\right) \qquad (3)$$

This is one of the two partial differential equations which describe in general terms the superheat region of the evaporator.

4.2 THERMAL ENERGY CONTENT OF ELEMENT

We will adhere to convention and consider all thermal energy relative to that of liquid ammonia at -40^0 F, (420^0 R). The use of any other datum would be just as satisfactory.

One must remember that thermal energy here represents the sum of the thermal energy contained in the evaporator material and in the ammonia vapour.

Thus, at time τ, the thermal energy content of an element is given by

$$Q = Cp_E \cdot \rho_E \cdot \left(T_v + \frac{\partial T_v}{\partial x} \cdot \frac{\Delta x}{2} - T_{420}\right) \cdot \left(A + \frac{\partial A}{\partial x} \cdot \frac{\Delta x}{2}\right) \Delta x$$

$$+ \frac{P \cdot \Delta x}{R\left(T_v + \frac{\partial T_v}{\partial x} \cdot \frac{\Delta x}{2}\right)} \cdot \left(A + \frac{\partial A}{\partial x} \cdot \frac{\Delta x}{2}\right) \cdot \left[L + Cp_v\left(T_v + \frac{\partial T_v}{\partial x} \cdot \frac{\Delta x}{2} - T_{420}\right)\right]$$

Similarly, at time $\tau + \Delta\tau$, the thermal energy content is given by

$$Q + \Delta Q = Cp_E \cdot \rho_E \cdot \left(T_v + \frac{\partial T_v}{\partial x} \cdot \frac{\Delta x}{2} + \frac{\partial T_v}{\partial \tau} \cdot \Delta\tau - T_{420} \right) \cdot \left(A + \frac{\partial A}{\partial x} \cdot \frac{\Delta x}{2} \right) \cdot \Delta x$$

$$+ \frac{\left(P + \frac{\partial P}{\partial \tau} \cdot \Delta\tau \right) \cdot \frac{\Delta x}{R} \cdot \left(A + \frac{\partial A}{\partial x} \cdot \frac{\Delta x}{2} \right)}{\left(T_v + \frac{\partial T_v}{\partial x} \cdot \frac{\Delta x}{2} + \frac{\partial T_v}{\partial \tau} \cdot \Delta\tau \right)} \cdot \left[L + Cp_v \left(T_v + \frac{\partial T_v}{\partial x} \circ \frac{\Delta x}{2} + \frac{\partial T_v}{\partial \tau} \cdot \Delta\tau - T_{420} \right) \right]$$

Hence, the increase in the thermal energy content of an element in time $\Delta\tau$ is given by the difference between the latter two expressions, which reduces to

$$\Delta Q = A \cdot \Delta x \circ \Delta\tau \left[Cp_E \cdot \rho_E \circ \frac{\partial T_v}{\partial \tau} + \frac{Cp_v}{R} \circ \frac{\partial P}{\partial \tau} + \frac{\left(L - Cp_v \circ T_{420} \right)}{R} \cdot \frac{\partial}{\partial \tau} \left(\frac{P}{T_v} \right) \right] \tag{4}$$

as $\Delta\tau$ and $\Delta x \longrightarrow 0$

The thermal energy content must now be considered on the basis of the rate of flow of thermal energy into the element. The flow of thermal energy into the element in time $\Delta\tau$ can be considered in three parts

$$\Delta Q = \Delta Q_1 + \Delta Q_2 + \Delta Q_3$$

where ΔQ_1 = axial thermal energy flow across the section at station x in time $\Delta\tau$

ΔQ_2 = axial thermal energy flow across the section at station x + Δx in time $\Delta\tau$

ΔQ_3 = radial thermal energy flow across the circumference of element Δx in time $\Delta\tau$.

The values ΔQ_1 and ΔQ_2 each represent the sum of the thermal energy flow due to the flow of ammonia and due to axial conduction. Thus, in general, the rate of axial thermal energy flow across a section is given by

$$q = \frac{P}{R \cdot T_v} \cdot A \cdot s \left[L + Cp_v \left(T_v - T_{420} \right) \right] - k_E \cdot A \cdot \frac{\partial T_v}{\partial x}$$

It should be noted that A has already been defined as the internal cross-sectional area of the evaporator but the same symbol is used here, remembering that k_E is the mean thermal conductivity of the cross-section.

One can then write

$$\Delta Q_1 = \frac{A\left[P \cdot s + \frac{\partial}{\partial \tau}(P \cdot s) \cdot \frac{\Delta \tau}{2}\right]}{R\left(T_v + \frac{\partial T_v}{\partial \tau} \cdot \frac{\Delta \tau}{2}\right)} \cdot \left[L + Cp_v\left(T_v + \frac{\partial T_v}{\partial \tau} \cdot \frac{\Delta \tau}{2} - T_{420}\right)\right] \cdot \Delta \tau$$

$$- k_E \circ A\left[\frac{\partial T_v}{\partial x} + \frac{\partial}{\partial \tau}\left(\frac{\partial T_v}{\partial x}\right) \cdot \frac{\Delta \tau}{2}\right] \Delta \tau$$

and

$$\Delta Q_2 = \left(A + \frac{\partial A}{\partial x} \cdot \Delta x\right)\left(P + \frac{\partial P}{\partial \tau} \cdot \frac{\Delta \tau}{2}\right)\left(s + \frac{\partial s}{\partial \tau} \cdot \frac{\Delta \tau}{2} + \frac{\partial s}{\partial x} \circ \Delta x\right) \cdot$$

$$\frac{\left[L + Cp_v\left(T_v + \frac{\partial T_v}{\partial \tau} \cdot \frac{\Delta \tau}{2} + \frac{\partial T_v}{\partial x} \cdot \Delta x\right)\right] \cdot \Delta \tau}{R\left(T_v + \frac{\partial T_v}{\partial \tau} \cdot \frac{\Delta \tau}{2} + \frac{\partial T_v}{\partial x} \cdot \Delta x\right)}$$

$$- k_E \cdot \left(A + \frac{\partial A}{\partial x} \cdot \Delta x\right) \cdot \left[\frac{\partial T_v}{\partial x} + \frac{\partial}{\partial \tau}\left(\frac{\partial T_v}{\partial x}\right) \cdot \frac{\Delta \tau}{2} + \frac{\partial}{\partial x}\left(\frac{\partial T_v}{\partial x}\right) \cdot \Delta x\right] \cdot \Delta \tau$$

For the rate of radial thermal energy flow, let us use the relationship

$$q = q_0 \left(T_{AMB} - T_v\right)$$

where q_0 is the rate of flow of thermal energy in a radial direction at the circumference of the evaporator at station x and time τ, measured in Btu/hr^{0}F foot length of evaporator. It will be more convenient to evaluate q_0 later in the analysis, and an expression is evaluated in section 5.7.

Then, over length Δx and time $\Delta\tau$ we can write

$$\Delta Q_3 = q_0 \cdot \Delta x \cdot \Delta\tau \left[T_{AMB} - \left(T_v + \frac{\partial T_v}{\partial\tau} \cdot \frac{\Delta\tau}{2} + \frac{\partial T_v}{\partial x} \cdot \Delta x \right) \right]$$

The sum, ΔQ, of the above three terms reduces to

$$\Delta Q = \Delta x \cdot \Delta\tau \left[-\frac{Cp_v}{R} \cdot P \cdot \frac{\partial}{\partial x} \left(A \cdot s \right) - \left(\frac{L - Cp_v \cdot T_{420}}{R} \right) \cdot P \cdot \frac{\partial}{\partial x} \left(\frac{A \cdot s}{T_v} \right) \right.$$

$$\left. + k_E \cdot A \cdot \frac{\partial^2 T_v}{\partial x^2} + k_E \frac{\partial A}{\partial x} \cdot \frac{\partial T_v}{\partial x} + q_0 \left(T_{AMB} - T_v \right) \right] \tag{5}$$

as $\Delta\tau$ and $\Delta x \longrightarrow 0$

Equations (4) and (5) must represent the same quantity, and thus can be equated. In the resulting expression, equation (3) can be used to eliminate a pair of terms and one obtains

$$A \cdot Cp_E \cdot \rho_E \cdot \frac{\partial T_v}{\partial\tau} + A \cdot \frac{Cp_v}{R} \cdot \frac{\partial P}{\partial\tau} = -\frac{P \cdot Cp_v}{R} \cdot \frac{\partial}{\partial x} \left(A \cdot s \right) + k_E \cdot A \cdot \frac{\partial^2 T_v}{\partial x^2}$$

$$+ k_E \cdot \frac{\partial A}{\partial x} \cdot \frac{\partial T_v}{\partial x} + q_0 \left(T_{AMB} - T_v \right) \tag{6}$$

This is the second of the two partial differential equations which describe the superheat region of the evaporator.

4.3 DERIVATION OF STEADY STATE EQUATION

Expanding equation (3) gives

$$A \left(-\frac{P}{{T_v}^2} \cdot \frac{\partial T_v}{\partial\tau} + \frac{1}{T_v} \cdot \frac{\partial P}{\partial\tau} \right) = -P \left[-\frac{A \cdot s}{{T_v}^2} \cdot \frac{\partial T_v}{\partial x} + \frac{1}{T_v} \cdot \frac{\partial}{\partial x} \left(A \cdot s \right) \right]$$

Multiplying through by $\dfrac{Cp_v}{R} \cdot T_v$ gives

$$-\frac{Cp_v}{R} \cdot \frac{A \cdot P}{T_v} \cdot \frac{\partial T_v}{\partial \tau} + \frac{Cp_v}{R} \cdot A \cdot \frac{\partial P}{\partial \tau} = \frac{Cp_v}{R} \cdot \frac{A \cdot s \cdot P}{T_v} \cdot \frac{\partial T_v}{\partial x} - \frac{Cp_v}{R} \cdot P \cdot \frac{\partial}{\partial x} \left(A \cdot s\right)$$

One can now substitute in equation (6) and reduce the latter to a partial differential equation containing differentials of T_v and A only :

$$A \cdot Cp_E \cdot \rho_E \cdot \frac{\partial T_v}{\partial \tau} + \frac{Cp_v}{R} \cdot \frac{A \cdot P}{T_v} \cdot \frac{\partial T_v}{\partial \tau} = -\frac{Cp_v}{R} \cdot \frac{A \cdot s \cdot P}{T_v} \cdot \frac{\partial T_v}{\partial x} + k_E \cdot A \cdot \frac{\partial^2 T_v}{\partial x^2}$$

$$+ k_E \cdot \frac{\partial A}{\partial x} \cdot \frac{\partial T_v}{\partial x} + q_0 \left(T_{AMB} - T_v\right) \qquad (6a)$$

The equation can be simplified by making A and P constant. One can justify these respective steps since it is our intention at this time to consider only evaporators of constant cross-section and the anticipated pressure variations will be small and of a relatively high frequency thus permitting the use of a mean pressure value for P without significant error.

One can then write (6a) in the form

$$\left(A \cdot Cp_E \cdot \rho_E\right) \frac{\partial T_v}{\partial \tau} + \left(\frac{Cp_v}{R} \cdot A \cdot P\right) \frac{1}{T_v} \cdot \frac{\partial T_v}{\partial \tau} + \left(\frac{Cp_v}{R} \cdot A \cdot P\right) \frac{s}{T_v} \cdot \frac{\partial T_v}{\partial x}$$

$$- \left(k_E \cdot A\right) \frac{\partial^2 T_v}{\partial x^2} + q_0 T_v - q_0 T_{AMB} = 0 \qquad (7)$$

As previously stated, only the steady state case will be considered. Hence time dependent terms vanish, leaving

$$k_E \cdot A \cdot \frac{\partial^2 T_v}{\partial x^2} - \frac{Cp_v}{R} \cdot A \cdot P \cdot \frac{s}{T_v} \cdot \frac{\partial T_v}{\partial x} - q_0 T_v = - q_0 T_{AMB}$$

Now, the mass flow rate is given by

$$m = \rho_v \cdot A \cdot s$$

$$= \frac{P}{R \cdot T_v} \cdot A \cdot s$$

Hence :

$$\frac{s}{T_v} = \frac{m \cdot R}{P \cdot A}$$

then

$$\frac{Cp_v}{R} \cdot A \cdot P \cdot \frac{s}{T_v} = \frac{Cp_v}{R} \cdot A \cdot P \cdot \frac{m \cdot R}{P \cdot A} = m \cdot Cp_v$$

= constant, for steady-state conditions.

One can now rewrite the above equation as

$$c_1 \frac{\partial^2 T_v}{\partial x^2} - c_2 \frac{\partial T_v}{\partial x} - c_3 T_v = - c_4 \qquad (8)$$

where

$$\left.\begin{aligned} c_1 &= k_E \cdot A \\ c_2 &= Cp_v \cdot m \\ c_3 &= q_0 \\ c_4 &= q_0 T_{AMB} \end{aligned}\right\} \text{constants of known value}$$

Equation (8) is the governing differential equation for steady state conditions in the superheat region. Equation (3) can be seen to be identically zero for the steady state.

4.4 SOLUTION OF STEADY STATE EQUATION

Solving equation (8) gives

$$T_v = K_1 e^{c_6 x} + K_2 e^{c_7 x} + \frac{c_4}{c_3} \qquad (9)$$

where

$$c_6 = \frac{c_2}{2 c_1} - \sqrt{\left(\frac{c_2}{2 c_1}\right)^2 + \frac{c_3}{c_1}} \qquad (10)$$

$$c_7 = \frac{c_2}{2\,c_1} + \sqrt{\left(\frac{c_2}{2\,c_1}\right)^2 + \frac{c_3}{c_1}} \tag{11}$$

and

$$\frac{c_4}{c_3} = T_{AMB}$$

K_1 and K_2 are constants of unknown value at this point.

Boundary conditions. Let us consider the zero of the x scale to be at the liquid boundary. Then the superheat region extends from $x = 0$ to $x = \lambda_s$ where λ_s is the length of the superheat region.

(a) When $x = 0$, $T_v = T_L$

Hence, $$T_L = K_1 + K_2 + T_{AMB} \tag{12}$$

(b) When $x = \lambda_s$, let us assume a relationship of the form

$$\frac{\partial T_v}{\partial x} = K_3 \left(T_{AMB} - T_v \right)$$

The value of K_3 depends on the exact conditions assumed at the end face. For example, if the face is insulated from the spacecraft structure, K_3 will equal zero.

One can write

$$K_3 \left(T_{AMB} - T_v \right) = c_6 K_1 e^{c_6 \lambda_s} + c_7 K_2 e^{c_7 \lambda_s}$$

i.e.

$$K_3 \left(- K_1 e^{c_6 \lambda_s} - K_2 e^{c_7 \lambda_s} \right) = c_6 K_1 e^{c_6 \lambda_s} + c_7 K_2 e^{c_7 \lambda_s}$$

$$K_1 e^{c_6 \lambda_s} \left(c_6 + K_3 \right) + K_2 e^{c_7 \lambda_s} \left(c_7 + K_3 \right) = 0$$

or

$$K_1 = - K_2 \left(\frac{c_7 + K_3}{c_6 + K_3} \right) e^{\left(c_7 - c_6 \right) \lambda_s}$$

Writing

$$c_6 + K_3 = c_8$$

$$c_7 + K_3 = c_9$$

and

$$c_7 - c_6 = c_{10}$$

and substituting for K_1 in equation (12) one obtains

$$T_L = -K_2 \left(\frac{c_9}{c_8}\right) e^{c_{10}\lambda_s} + K_2 + T_{AMB}$$

Hence

$$K_2 = \frac{T_{AMB} - T_L}{\frac{c_9}{c_8} e^{c_{10}\lambda_s} - 1}$$

and

$$K_1 = \frac{T_{AMB} - T_L}{\frac{c_8}{c_9} e^{-c_{10}\lambda_s} - 1}$$

Then, equation (9) can be rewritten as

$$T_v = T_{AMB} - \left(T_{AMB} - T_L\right)\left(\frac{e^{c_6 x}}{1 - \frac{c_8}{c_9} e^{-c_{10}\lambda_s}} + \frac{e^{c_7 x}}{1 - \frac{c_9}{c_8} e^{c_{10}\lambda_s}}\right) \qquad (13)$$

It must be remembered that this relation applies only to the superheat region of the evaporator. In the boiling region $T_v = T_L$.

Unless λ_s is very small compared with the evaporator diameter, the quantity $\frac{c_9}{c_8} e^{c_{10}\lambda_s}$ will be much larger than unity and one can write

$$T_v = T_{AMB} - \left(T_{AMB} - T_L\right)\left(e^{c_6 x} - \frac{e^{c_7 x}}{\frac{c_9}{c_8} e^{c_{10}\lambda_s}}\right) \qquad (14)$$

The type of curve represented by equation (14) is shown in Fig. 4 for typical low flow rate and high flow rate cases with various boundary conditions.

5. STEADY STATE HEAT EXCHANGE BETWEEN EVAPORATOR AND SPACECRAFT

It will be found that many watts of thermal power need to be supplied to the evaporator. As already stated in Section 1, the evaporator will obtain heat from the bulk of the spacecraft and the mechanism involved in this heat exchange must now be examined.

It is important to note that the spacecraft is intended to act as a heat sink (or more appropriately as a cold sink), thus favouring location of the evaporator at the centre of the spacecraft.

There are various well-known spacecraft applications which require part or all of the vehicle to be sun-pointing. In such cases it may well be beneficial to position the evaporator externally so that it will receive heat by direct radiation from the sun. In general, however, this application would result in a different type of evaporator which probably would not employ the metal sponge filling. Consequently, this type of application will not be considered here and it will be assumed that the evaporator is located at the centre of the spacecraft.

Since the spacecraft will normally not be pressurized and will be in free fall, there will be no contained gas nor gravity to support convective heat transfer. One must therefore rely on radiation and conduction through the structure to warm the evaporator.

5.1 HEATING BY RADIATION

As explained in section 3.1 the evaporator will be cylindrical in shape.

The radiative heat transfer between unit area of evaporator wall at temperature T_W and the surroundings at temperature T_{AMB} is given by the familiar type of expression

$$q_R = \sigma \cdot \epsilon \left(T_{AMB}^{\ 4} - T_w^{\ 4} \right)$$

where $$\sigma = 1.73 \times 10^{-9} \ \text{Btu/ft}^2 \ \text{hr}(^0\text{F})^4$$

If $T_{AMB} - T_w$ is small, one can write

$$T_w = T_{AMB} - \Delta T_{AMB}$$

Then

$$T_w^{\ 4} = T_{AMB}^{\ 4} - 4\,T_{AMB}^{\ 3} \cdot \Delta T_{AMB}$$

— ignoring higher powers of ΔT_{AMB}

and

$$\left(T_{AMB}^{\ 4} - T_w^{\ 4} \right) = 4\,T_{AMB}^{\ 3} \left(T_{AMB} - T_w \right)$$

One can also write

$$\epsilon = 1.0$$

thus permitting the greatest possible heat exchange, and

$$T_{AMB} = 70^0 \ \text{F} = 530^0 \ \text{R}$$

The equation then reduces to

$$q_R = 1.03 \left(T_{AMB} - T_w \right) \ \text{Btu/ft}^2 \ \text{hr}$$

5.2 HEATING BY CONDUCTION

Let us initially consider the simple case of a small sphere of radius r_{SPH} located at the centre of, and exchanging heat by conduction with, a large homogeneous sphere of radius r_{SC} which represents the spacecraft, as shown in Fig. 5.

The traditional partial differential equation for transient conduction through a three dimensional solid is

$$\frac{\partial^2 T}{\partial x^2} + \frac{\partial^2 T}{\partial y^2} + \frac{\partial^2 T}{\partial z^2} = \alpha^2 \cdot \frac{\partial T}{\partial \tau}$$

where

$$\alpha^2 = \frac{Cp \cdot \rho}{k}$$

By transforming to spherical co-ordinates and attaching the subscript sc to indicate spacecraft parameters, one can show that for concentric thermally symmetric spheres the equation becomes

$$\frac{\partial^2 T_{SC}}{\partial r^2} + \frac{2}{r} \cdot \frac{\partial T_{SC}}{\partial r} = \alpha^2 \cdot \frac{\partial T_{SC}}{\partial \tau} \tag{15}$$

where

$$\alpha^2 = \frac{Cp_{SC} \cdot \rho_{SC}}{k_{SC}}$$

For the steady state case

$$\frac{\partial^2 T_{SC}}{\partial r^2} + \frac{2}{r} \cdot \frac{\partial T_{SC}}{\partial r} = 0$$

Solving this equation gives the general relationship

$$T_{SC} = K_1 - \frac{K_2}{r}$$

Applying boundary conditions

when

$$r = r_{SC}, \qquad T_{SC} = T_{AMB}$$

and when

$$r = r_{SPH}, \qquad T_{SC} = T_w$$

one obtains

$$T_{SC} = T_{AMB} + (T_{AMB} - T_w) \cdot \frac{r_{SPH}}{(r_{SC} - r_{SPH})} \cdot \left(1 - \frac{r_{SC}}{r}\right) \tag{16}$$

Also

$$\frac{\partial T_{SC}}{\partial r} = (T_{AMB} - T_w) \cdot \frac{r_{SPH}}{r_{SC} - r_{SPH}} \cdot \frac{r_{SC}}{r^2} \tag{16a}$$

It should be noted that this use of T_{AMB} as the temperature at the periphery of the spacecraft is a slight distorsion of the literal truth, since one would normally regard T_{AMB} as the mean temperature of the spacecraft. However, inspection of the derived temperature variation through the spacecraft shows very little difference between these two temperatures, and it is quite acceptable and indeed very convenient to define T_{AMB} in this way. When $r = r_{SPH}$

$$\left(\frac{\partial T_{SC}}{\partial r}\right)_{r_{SPH}} = (T_{AMB} - T_w) \cdot \frac{r_{SC}}{r_{SC} - r_{SPH}} \cdot \frac{1}{r_{SPH}}$$

and if r_{SC} is much greater than r_{SPH} (a valid assumption)

$$\left(\frac{\partial T_{SC}}{\partial r}\right)_{r_{SPH}} = \frac{T_{AMB} - T_w}{r_{SPH}} \tag{17}$$

Then, the conductive heating rate to a small sphere per unit area is given by

$$q_C = k_{SC} \left(\frac{\partial T_{SC}}{\partial r}\right)_{r_{SPH}}$$

$$= k_{SC} \cdot \frac{(T_{AMB} - T_w)}{r_{SPH}}$$

We need to insert some typical values for k_{SC} and r_{SPH}. If actual spacecraft structures are examined they will be seen typically to be constructed of aluminium or magnesium alloy with an overall density roughly 1/30 to 1/60 of that of the solid metal. The value of k for aluminium alloy is about 120 Btu/hr ft ^{0} F. Hence, an effective k_{SC} in the range 2.0 to 4.0 would be typical. Magnesium alloy would be very similar. Stainless steel would reduce k_{SC} very considerably, but it is not a popular material for such structures. It should be noted that we have only considered the conductivity of the structure, since the spacecraft payload, although contributing considerable mass, is not likely to add much to the thermal conduction path through the structure.

To obtain a typical value for r_{SPH} one can predict intuitively that anything larger than a 4 inch diameter sphere (say) would be too massive for consideration. Therefore $r_{SPH} = 0.167$ ft will give an upper limit for radius.

Then, one will obtain a low value for q_C if one writes

$$q_C = \frac{2.0}{0.167}\left(T_{AMB} - T_w\right) = 12.0\left(T_{AMB} - T_w\right) \qquad \text{Btu/ft}^2\text{ hr}$$

5.3 COMPARISON OF RADIATIVE AND CONDUCTIVE HEAT EXCHANGE

One can see immediately that the use of the most pessimistic figure for conduction still results in a heat exchange value 12 times greater than that obtainable by radiation.

It seems reasonable to ignore the effect of radiation and therefore only the effect of conduction will be considered in the following analysis.

5.4 CONDUCTIVE HEAT EXCHANGE APPLIED TO A CYLINDRICAL EVAPORATOR

It would normally not be difficult to provide locally better conduction than indicated by the values suggested in section 5.2. Appropriate design or location of the evaporator could easily improve k_{SC} locally to a value of 5.0 Btu/ft hr ^{0} F.

Location of the evaporator close to a heat source such as a battery will obviously be beneficial but all spacecraft equipment (and batteries especially) will have restricted operating temperature limits and will themselves undoubtedly rely on conduction into the general spacecraft structure to dissipate their heat. Attempting to directly balance a cold source and a hot source is almost unthinkable except in the case of the thruster system components which will generate only a few watts. In this analysis, therefore, one would expect no benefit from hot sources.

Returning to section 5.2 and the analysis of heat transfer between concentric homogeneously conducting spheres, equation (17) was obtained for the steady state radial temperature gradient at the surface of the inner sphere i.e.

$$\left(\frac{\partial T_{SC}}{\partial r}\right)_{r_{SPH}} = \frac{T_{AMB} - T_W}{r_{SPH}}$$

For a non-spherical small body let us say that the mean temperature gradient normal to its surface is given by the same equation, where r_{SPH} is now the radius of some "equivalent sphere".

The equivalent sphere can be defined as the sphere having the same volume or same surface area as the small body (evaporator). It is not the intention of this study to investigate this aspect in quantitative detail. Inspection alone suggests that a sphere having the same surface area will be a reasonable basis for an equivalent sphere. Accordingly, for a cylindrical evaporator of radius r_E and length λ_T, one can write approximately

$$4\pi\ r_{SPH}{}^2 = 2\pi\ r_E{}^2 + 2\pi\ r_E \cdot \lambda_T$$

This statement is approximate because λ_T is strictly measured internally. However the evaporator walls will be thin and the error incurred will be insignificant.

Writing $2r_E = d =$ cylindrical diameter of evaporator one obtains

$$r_{SPH} = r_E \sqrt{0.5 + \frac{\lambda_T}{d}} \tag{18}$$

5.5 HEAT TRANSFER TO BOILING REGION

The external surface area of the boiling region is approximately

$$\pi r_E^{\,2} + 2\pi r_E \cdot \lambda_B$$

and the heating rate to this region from the surroundings is given by

$$q_{B1} = k_{SC} \left(\pi r_E^{\,2} + 2\pi r_E \cdot \lambda_B \right) \cdot \left(\frac{\partial T_{SC}}{\partial r} \right)_{r_{SPH}}$$

$$= 4\pi r_E^{\,2} \cdot k_{SC} \left(0.25 + \frac{\lambda_B}{d} \right) \left(\frac{T_{AMB} - T_W}{r_{SPH}} \right)$$

But, in the boiling region as explained in section 3.3 (a) $\quad T_W = T_L$

Hence

$$q_{B1} = 4\pi k_{SC} \cdot r_E \left(T_{AMB} - T_L \right) \frac{\left(0.25 + \frac{\lambda_B}{d} \right)}{\sqrt{0.5 + \frac{\lambda_T}{d}}}$$

Also the axial heating rate to the boiling region from the superheat region is given by

$$q_{B2} = k_E \cdot A \left(\frac{\partial T}{\partial x} \right)_{x\,=\,0}$$

where $k_E \cdot A = c_1$ as defined in equation (8)
and using equation (14)

$$\left(\frac{\partial T}{\partial x} \right)_{x\,=\,0} = \left(T_{AMB} - T_L \right) \cdot \left(- c_6 + \frac{c_7\, c_8}{c_9\, e^{\,c_{10} \lambda_s}} \right)$$

At this stage we will make the simplifying assumption that the outlet end face of the evaporator is insulated from the spacecraft structure.

Since it is our intention to warm this end of the evaporator to near ambient temperature, one would expect very little heat transfer at this point anyway and inspection shows that different boundary conditions at this end have negligible effects on the resulting ammonia outlet temperature. Fig. 4 illustrates this point.

Referring to section 4.4, the constant K_3 therefore becomes zero, and

$$c_8 = c_6$$

$$c_9 = c_7$$

so that

$$\left(\frac{\partial T}{\partial x}\right)_{x=0} = \left(T_{AMB} - T_L\right) \cdot c_6 \cdot \left(-1 + \frac{1}{e^{c_{10}\lambda_s}}\right)$$

but it will be found that, in all practical cases, the quantity

$$e^{-c_{10}\lambda_s}$$

will be very small indeed and much less than unity.

Hence

$$q_{B2} = - c_1 c_6 \left(T_{AMB} - T_L\right)$$

Then, the total rate of heat transfer to the boiling region is given by

$$q_B = q_{B1} + q_{B2}$$

or

$$q_B = \left(T_{AMB} - T_L\right) \left[4\pi k_{SC} r_E \frac{\left(0.25 + \frac{\lambda_B}{d}\right)}{\sqrt{0.5 + \frac{\lambda_T}{d}}} - c_1 c_6\right]$$

But the heating rate required to evaporate the ammonia is given by

$$q'_B = m \left[(h + L) - h_{AMB} \right]$$

where h is the mean enthalpy of liquid ammonia over the range of temperatures corresponding to the range of internal pressures in the evaporator and h_{AMB} is the enthalpy of liquid ammonia at the ambient temperature.

Let us write

$$q'_B = m \cdot \Delta H_B$$

Then one can equate

$$q_B = q'_B$$

Hence

$$\frac{0.25 + \dfrac{\lambda_B}{d}}{\sqrt{0.5 + \dfrac{\lambda_T}{d}}} = \left(\frac{m \cdot \Delta H_B}{T_{AMB} - T_L} - c_1 c_6 \right) \cdot \frac{1}{4\pi k_{SC} \cdot r_E} \tag{19}$$

5.6 HEAT TRANSFER TO SUPERHEAT REGION

We have already derived equation (14) which represents the temperature variation through the superheat region.

One of the significant parameters in designing an evaporator for a given application is the ultimate temperature of the gaseous ammonia at the outlet, i.e. the value of T_V when $x = \lambda_S$, which will be designated as T_{ULT}.

Using equation (14) and remembering that $c_8 = c_6$ and $c_9 = c_7$

$$T_{ULT} = T_{AMB} - (T_{AMB} - T_L) \left(e^{c_6 \lambda_s} - \frac{e^{c_7 \lambda_s}}{\dfrac{c_7}{c_6} e^{c_{10} \lambda_s}} \right)$$

or

$$\frac{T_{AMB} - T_{ULT}}{T_{AMB} - T_L} = e^{c_6 \lambda_s} \left(1 - \frac{c_6}{c_7}\right)$$

Referring to Fig. 17 for notation, and rearranging, one obtains

$$\lambda_s = \frac{\text{Log}_e \left[\frac{\Delta T_0}{\Delta T} \left(1 - \frac{c_6}{c_7}\right)\right]}{- c_6} \tag{20}$$

The total length of the evaporator is then given by

$$\lambda_T = \lambda_B + \lambda_s \tag{21}$$

5.7 CONSTANTS c_1, c_2 AND c_3

The constants c_1, c_2 and c_3 defined in equation (8) now need to be considered in greater detail.

c_1 : In the particular case of a cylindrical evaporator filled with nickel sponge material, we have

$$c_1 = 2\pi r_E \left(k_w \cdot t_w + \frac{k_F \cdot r_E}{2}\right) \tag{22}$$

where k_F = thermal conductivity of the nickel sponge material

k_w = thermal conductivity of the wall material

t_w = thickness of the wall

It should be remembered that r_E is the outside radius of the evaporator. However, t_w will be small, and the above use of r_E will only introduce a negligible error.

c_2 : The original definition needs no elaboration

$$c_2 = Cp_v \cdot m \tag{23}$$

c_3 : according to equation (8)

$$c_3 = q_0$$

= rate of flow of thermal energy in a radial direction at the circumference of the evaporator per unit length of the evaporator per hr.^{0}F.

The radial heating rate per unit *area* per hr is given by

$$q_A = k_{SC} \cdot \frac{\partial T_{SC}}{\partial r}$$

but, for the superheat region

$$\frac{\partial T_{SC}}{\partial r} = \frac{T_{AMB} - T_W}{r_E \sqrt{0.5 + \frac{\lambda_T}{d}}}$$

Then, the radial heating rate per unit *length* of the cylindrical wall per hr per ^{0}F of temperature difference between the ambient and ammonia vapour temperatures is given by

$$q_0 = q_A \times \frac{\text{circumference}}{\text{temperature difference}}$$

$$= \frac{k_{SC} \cdot (T_{AMB} - T_W)}{r_E \sqrt{0.5 + \frac{\lambda_T}{d}}} \cdot \frac{2\pi r_E}{T_{AMB} - T_V}$$

Now, according to the result in Appendix I

$$\frac{T_{AMB} - T_W}{T_{AMB} - T_V} = \frac{4 k_F}{4 k_F + k_{SC}}$$

Hence

$$c_3 = q_0$$

$$= \frac{8\pi \left(\frac{k_{SC} \cdot k_F}{k_{SC} + 4 k_F} \right)}{\sqrt{0.5 + \frac{\lambda_T}{d}}} \tag{24}$$

6. APPLICATION OF THE STEADY STATE ANALYSIS

Since there are at least 9 independent variables defining the operating conditions in the evaporator, a general analytical solution for selection of the best evaporator shape in terms of those variables is almost impossible. In any case, more can be learned about the dependence of the system on the various parameters by evaluating each case numerically as will be demonstrated in this and the following chapter.

6.1 METHOD OF EVALUATING THE LENGTH OF THE EVAPORATOR

The foregoing analysis can be used to evaluate the length of evaporator required for given conditions and for a given radius, as follows.

Values are first required for the following parameters :

P - mean internal pressure in the evaporator

T_{AMB} - ambient temperature of surroundings (spacecraft)

T_{ULT} - required temperature of ammonia vapour at exit

k_{SC} - effective thermal conductivity of spacecraft structure

k_F - effective thermal conductivity of nickel sponge material

k_W - thermal conductivity of evaporator wall material

t_W - thickness of evaporator wall

m - mass flow rate of ammonia

r_E - external cylindrical radius of evaporator

The following quantities can then be evaluated :

Cp_v - specific heat of ammonia vapour at mean internal pressure, from ammonia tables

T_L - temperature of boiling liquid ammonia at mean internal pressure, from ammonia tables

ΔH_B - enthalpy rise of ammonia in boiling region, evaluated at the mean internal pressure, from ammonia tables

$$\frac{\Delta T_0}{\Delta T} = \frac{T_{AMB} - T_L}{T_{AMB} - T_{ULT}}$$

One then has eight equations to evaluate

$$c_1 = 2\pi r_E \left(k_w \cdot t_w + \frac{k_F \cdot r_E}{2} \right) \tag{22}$$

$$c_2 = Cp_v \cdot m \tag{23}$$

$$c_3 = \frac{8\pi \left(\dfrac{k_{SC} \cdot k_F}{k_{SC} + 4 k_F} \right)}{\sqrt{0.5 + \dfrac{\lambda_T}{d}}} \tag{24}$$

$$c_6 = \frac{c_2}{2 c_1} - \sqrt{\left(\frac{c_2}{2 c_1}\right)^2 + \frac{c_3}{c_1}} \tag{10}$$

$$c_7 = \frac{c_2}{2 c_1} + \sqrt{\left(\frac{c_2}{2 c_1}\right)^2 + \frac{c_3}{c_1}} \tag{11}$$

$$\frac{0.25 + \dfrac{\lambda_B}{d}}{\sqrt{0.5 + \dfrac{\lambda_T}{d}}} = \left(\frac{m \cdot \Delta H_B}{T_{AMB} - T_L} - c_1 c_6 \right) \cdot \frac{1}{4\pi k_{SC} \cdot r_E} \tag{19}$$

$$\lambda_s = \frac{\mathrm{Log}_e \left[\dfrac{\Delta T_0}{\Delta T} \left(1 - \dfrac{c_6}{c_7} \right) \right]}{- c_6} \tag{20}$$

$$\lambda_T = \lambda_B + \lambda_s \tag{21}$$

It is evidently not possible to solve explicitly for λ_B and λ_s, and an iterative process is required. Fortunately this technique lends itself readily to solution by a digital computer.

A programme has been written which starts by assuming a value of 0.5 ft for λ_T so that initial values can be calculated for c_3 and c_6.

Equations (19) and (20) are used to obtain values for λ_B and λ_s respectively.

Equation (21) gives an improved value for λ_T, and so on until the required accuracy is achieved.

6.2 CRITERIA FOR SELECTION OF THE BEST EVAPORATOR SHAPE

One requires a means of deciding the "best" radius and corresponding length of evaporator for a given application. Criteria which might determine the best shape are weight, internal plenum volume and dimension in a given direction. Any one of these factors may have priority in a given application and we will consider the variation of all three when presenting the results of the case study in the following section. The calculation of weight and volume are trivial computations easily added to the computer programme described in section 6.1.

7. SAMPLE CASE STUDY OF SIMPLE EVAPORATOR

7.1 SELECTION OF PARAMETER VALUES

It is required to assign typical parameter values which will represent a realistic application. A range of values of evaporator diameter and nickel sponge density will be considered and graphs will be obtained showing the weight and length of the evaporator as functions of these variables.

Parameter values were selected as follows :

P = 20 lb/in^2 absolute

T_{AMB} = 32^0F. This figure is slightly lower than the low ambient temperature limit for most spacecraft.

T_{ULT} = Rather than specify a value for this parameter as such, one can stipulate that :

$$\frac{\Delta T_0}{\Delta T} = 10$$

i.e. the difference between the ammonia vapour and ambient temperatures at the outlet is one tenth of the difference between the boiling ammonia and ambient temperatures. It can then be shown, having obtained a value for T_L, that $T_{ULT} = 27.1^0$F.

k_{SC} = 4.0 Btu/hr ft ^{0}F. According to the discussion in section 5.2 this value represents a high limit for average spacecraft structures. However, it should be easily attainable by appropriate design when required.

k_W = 12.0 Btu/hr ft ^{0}F. This is a typical value for stainless steel which is the assumed wall material.

t_w = 0.020 in. Strength requirements could be satisfied with a thinner skin, but fabrication difficulties could then become prohibitive.

m = 10^{-4} lb/s. This rate of flow is typical of the applications for which the system is intended.

r_E = Values covering the range 0.15 to 2.0 inches will be considered.

k_F = Values of sponge density covering the range from 0.25 to 16.0 percent will be considered. Since the thermal conductivity of solid nickel is 36 Btu/hr ft ^{0}F, the range of values of thermal conductivity is from 0.09 to 5.76 Btu/hr ft ^{0}F.

For the evaluation of the weight, density figures of 485 lb/ft^3 for stainless steel and 540 lb/ft^3 for solid nickel were utilized.

Values were then obtained for the additional parameters, as follows :

Cp_v = 0.5 Btu/lb ^{0}F, from tables.

T_L = – 16.9^{0}F, from tables.

$$\Delta H_B = h + L - h_{AMB} \text{ as defined in section 5.5.}$$

$$= 24.75 + 581.35 - 76.9, \text{ from tables.}$$

$$= 529.2 \text{ Btu/lb.}$$

$$\frac{\Delta T_0}{\Delta T} = 10.0 \text{ as already specified.}$$

7.2 RESULTS

The values selected in the previous section were inserted in the computer programme described in section 6.1, the resulting output being shown in Figs. 6 and 7.

Fig. 6 shows that curves of evaporator length as functions of sponge density yield minima, while variation of diameter at a given density also yields a minimum type of curve. If the overall minimum curve is plotted as shown by the dotted line, it is evident that evaporator length never falls below six inches.

Fig. 7 is of greater significance since it shows that for each given diameter, the variation of the sponge density yields a definite minimum of weight, but reduction of the evaporator diameter always causes a drop in weight with no apparent minimum. If the minimum points of the family of curves are joined as shown, the resulting curve appears to be asymptotic to the horizontal axis.

The implication is that the lowest evaporator weight will be obtained by reducing the diameter to a capillary size, with a length of several feet, perhaps. With such tubing the wall thickness could be considerably reduced from the adopted figure of 0.020 inches and even further weight reduction would result.

However, there are additional factors to bear in mind at this point. At the smallest diameters included on the graphs, the validity of the theory and the usefulness of the metal sponge becomes rather doubtful and extrapolation of the curves to even smaller diameters is not realistic. The installation of a long tubular evaporator in the spacecraft may also present problems of accessibility and integration with the structure and equipment, and it will not favour packaging of the thruster system in a desirable compact unit unless the tube is bent into a more convenient and less efficient shape. Furthermore, in a long thin evaporator the contained volume will be very drastically reduced as shown in Fig. 12. This is important since one of the functions of the evaporator is to act as a plenum chamber as explained in section 2.5. Several cubic inches of internal volume will be required and this factor alone tends to make a capillary tube type of evaporator unacceptable.

7.3 DISCUSSION

As a consequence of the results so far obtained, the following general requirements for evaporator design can be stated.

(a) The effective axial conduction path should be as small as possible, i.e. c_1 should be as small as possible. This implies a small effective cross-sectional area and requires that the evaporator mounting flanges should run radially rather than axially.

(b) The effective radial conduction path should be as large as possible, i.e. c_3 and λ_T and hence k_{SC} should be as large as possible.

Without resorting to the capillary size of tube, at least two possible ways of partially achieving these aims can be envisaged. One method would be to replace the sponge by a succession of metal screens or grids, each separated by a small axial distance. This device would preserve radial conduction but would considerably reduce the axial conduction path and thus comply with requirement (a).

A better method of construction which would comply with both requirements (a) and (b) is explored in Chapter 8.

8. THE DOUBLE-WALLED EVAPORATOR

Reference to Fig. 8 will clarify the discussion. An inner wall or baffle is now added to the simple evaporator and the fluid is forced to flow in the gap between the walls until it reaches the outlet end. The entire volume of the cylinder is still available as a reservoir, but the metal sponge is no longer needed throughout the core of the inner wall.

A small length of sponge will be retained however at the outlet end of the core, as shown in the figure. The intention is to minimize mixing of the flowing superheated vapour with the cold vapour which settles in the core. Such mixing would otherwise lower the temperature of the output vapour and reduce the efficiency of operation. In addition to the saving of weight obtained by removing most of the sponge, the effective conducting cross-section will be considerably reduced, the cross-section of the length retained being ignored, since axial temperature gradients are small in that area. We will make the retained length equal to one-fifth of the total evaporator length.

The sponge between the walls is also retained to aid heating of the ammonia and hold the liquid ammonia in its pores. An additional benefit of this type of construction is that accumulation of liquid ammonia will be severely restricted by the limited volume available in the boiling region.

8.1 CHANGES REQUIRED IN THE ANALYSIS

The basic analysis will still apply, but the values of c_1 and c_3 need to be altered.

If the thickness of the inner wall is the same as that of the external wall, t_W, and the thickness of the gap between them is t_G, we can write

$$c_1 = k_W \left[2\pi r_E \cdot t_W + 2\pi t_W \left(r_E - t_G - 2\,t_W \right) \right] + k_F \left[\pi \left(r_E - t_W \right)^2 - \pi \left(r_E - t_W - t_G \right)^2 \right]$$

Since the gap, t_G, will be small, one can assume uniform temperature in a radial direction, i.e., $T_w = T_v$ and c_3 becomes simply

$$c_3 = \frac{2\pi k_{sc}}{\sqrt{0.5 + \frac{\lambda_T}{d}}}$$

The expression for the evaporator weight must similarly be modified.

8.2 SAMPLE CASE STUDY OF THE DOUBLE-WALLED EVAPORATOR

Identical parameter values are specified as for the sample study of the simple evaporator in section 7, with the addition of the value

$$t_G = 0.1 \text{ inches}$$

8.3 RESULTS

The output from the computer programme for the double-walled evaporator is shown in Figs. 9 and 10.

In contrast to Figs. 6 and 7, Figs. 9 and 10 display no minima on the respective curves of evaporator length and evaporator weight as functions of sponge density. It is evident however that the lowest weight is given by the lowest possible sponge density and again by the lowest possible diameter, and the remarks of section 7.2 should again be borne in mind.

The depicted variation of length and weight at low values of sponge density is somewhat suspect and has been shown by broken lines, since the assumption of zero radial temperature gradient in the boiling and superheat regions may lose validity when the sponge conductivity is extremely low. On the other hand, the effect of convective heat transfer which previously has been ignored will then become more significant, and the net effect is indeterminate without more detailed work. However the low density range is not of great importance since densities below two percent are not commercially available, to this author's knowledge at the time of writing (1967).

The area of greatest interest is the density range of two to four percent, such material being readily available, and this region is examined in greater detail in Fig. 11 which compares the weight of simple and double walled evaporators as functions of diameter. It can be seen that for evaporator diameters greater than one and a half to two inches, the double walled evaporator is lighter than the simple type, whereas for lesser diameters, the double walled evaporator is slightly heavier.

However, Fig. 12, which compares the total volume of simple and double walled evaporators at sponge densities of two and four percent, shows that the double walled type is always more compact for a given diameter.

8.4 DISCUSSION

The situation is complex and the choice of evaporator shape and type would depend on the relative importance of evaporator weight, volume, length and permissible liquid accumulation. To illustrate this point, let us assume that one has a nickel sponge material with a density of two percent, and that the plenum requirement is for a volume of five cubic inches. Fig. 12 gives required diameters of 0.925 inches and 1.055 inches respectively for the simple and double walled types and Fig. 11 then gives respective weights of 0.170 pounds and 0.225 pounds, while Figs. 6 and 9 give respective lengths of 8.13 and 6.15 inches. Hence the double walled type, which of course exerts much greater control over liquid accumulation, will be shorter but heavier than the simple evaporator of the same volume.

Without further knowledge of the detailed system requirements, there is no clear superiority of either type of evaporator in this particular application. In other applications, one or other of the types may prove superior but each case must be examined quantitatively. Some improvement to the double walled type could be effected by reducing the inner wall thickness or making the inner wall from some such material as Teflon which would reduce both the overall weight and the conducting cross section.

9. EXPERIMENTAL CORRELATION

In order to demonstrate the validity of the steady state theory, a double walled evaporator was constructed and an experiment was set up, the results being compared with the calculated figures.

It should be noted that for a truly realistic appraisal, the experiment should be conducted in a vacuum and under zero "g" conditions in order to eliminate heat transfer due to atmospheric convection and condensation of atmospheric water vapour and to eliminate the influence of gravity on the liquid boundary shape and position. Since vacuum facilities were not available and zero "g" simulation would not be possible for the periods required, the work was conducted on the laboratory bench with precautions being taken as described in the following section.

9.1 APPARATUS

The general layout of the system was made as simple as possible, and is shown in Fig. 13, which may be compared with the layout of the typical thruster hardware shown in Fig. 1.

The evaporator was housed at the centre of a sheet aluminium structure, referred to as the dummy spacecraft. The thruster orifice was represented by a fine control metering valve with micrometer handle for precise re-setting. Neither pressure regulator nor stop valve were used in the line from the evaporator. Control of evaporator pressure was provided by a pressure switch mounted from a 4 – way connector upstream of the evaporator and operating a solenoid valve via a relay and 24 volt power supply.

A disused oxygen tank formed the supply reservoir for the liquid anhydrous ammonia, being connected directly to the solenoid valve inlet.

Steel or stainless steel were used for all metal parts in contact with ammonia.

The dummy spacecraft was constructed of 0.10 inch aluminium alloy sheet in the form of a large 2 foot cube joined by webs to a small 6 inch cube, the whole being bolted together and having an overall thermal conductivity representative of spacecraft structures. External joints were sealed with tape to minimise convective heat transfer. The small cube formed a housing for the evaporator, which was made from mild steel and bolted in place with the axis mounted vertically, the inlet being at the bottom, so as to minimise the effect of gravity on the liquid/vapour interface shape and position. The arrangement was intended to allow installation of different sizes of evaporator, and the mild steel evaporator flanges were therefore quite massive in order to preserve the continuity of conductivity in the less conductive material. The walls of the evaporator were also relatively massive to ease construction by welding.

Essential dimensions of the evaporator are shown in Fig. 14.

Instrumentation included 8 probe-type copper-constantan thermocouples mounted through the evaporator end wall and measuring the sponge/vapour temperature in the region between the double walls and one similar thermocouple measuring temperature within the outlet pipe. Thirteen surface-type copper-constantan thermocouples were mounted externally on the evaporator and on the dummy spacecraft. Thermocouple readings were obtained via a multiway switch and potentiometer. A bourdon type pressure gauge measured evaporator pressure and the flow rate was estimated by accurately weighing the ammonia container before and after a timed run of at least 2 hours duration.

9.2 METHOD

a) For each of six different orifice settings, and hence different flow rates, steady state axial temperature profiles were obtained for the evaporator. Graphs were then drawn of length of the boiling region, λ_B, and ultimate superheat temperature, T_{ULT}, on a base of flow rate.

b) Using the steady state analysis, estimates were made of the theoretical values of λ_B and T_{ULT} for each of the six sets of operating conditions observed in part (a) and corresponding graphs were drawn.

9.3 SYSTEM PARAMETER VALUES

The fixed parameters were as follows

Spacecraft thermal conductivity, k_{SC} = 6.0 Btu/ft hr ^{0}F.

This value was obtained by considering the weight of aluminium and mild steel contained in the given volume, using k = 120 for aluminium and k = 26 for mild steel.

Nickel sponge thermal conductivity, k_F = 1.39 Btu/ft hr ^{0}F.

This value represents the product of solid nickel thermal conductivity, 36 Btu/ft hr ^{0}F, and the measured density of the sponge material used, 3.86 $^0/_0$.

Wall thermal conductivity, k_W = 26 Btu/ft hr ^{0}F

Wall thickness, t_W = 0.125 inches

Gap thickness, t_G = 0.125 inches

External radius, r_E = 1.1775 inches

Total internal length, λ_T = 4.85 inches

Each of the six runs produced slightly different values for the remaining parameters, due partly to varying room temperature and partly to the varying flow rate itself. Ranges of values obtained for those parameters were as follows

Flow rate, m = 1.372×10^{-4} to 2.285×10^{-4} lb/s

Temperature at skin of dummy spacecraft, T_{AMB} = 60.0^0 to 69.5^{0}F

Mean internal pressure in evaporator, P = 11.25 to 12.5 lb/in^2 gauge

Temperature of boiling ammonia, T_L = – 7.8 to – 4.8^{0}F

Enthalpy rise in boiling region, ΔH_B = 479.35 to 486.4 Btu/lb

9.4 RESULTS

Fig. 15 compares the theoretical and measured variations of boiling length as functions of flow rate. It can be seen that although the agreement is good at large rates of flow, when the liquid boundary is well advanced up the evaporator, the agreement is poor at low flow rates. This discrepancy can be attributed to the assumptions leading up to equation (18) for the radius of the equivalent sphere. It will be remembered that the equivalent sphere was assumed to be the sphere having the same surface area as the evaporator. Judging by the results, a better criterion for the equivalent sphere would be the sphere having the same surface area as the boiling region of the evaporator. The computed heat transfer to the boiling region would then become greater especially for short boiling region lengths, thus leading to a reduction in the theoretical length.

Fig. 16 compares the theoretical and measured variations of the ultimate vapour temperature as functions of flow rate. It is evident that theory overestimates the ultimate temperature by 9 to 10^{0}F, throughout the range considered, in spite of the generally shorter superheat length available in the theoretical model. This behaviour is almost certainly due to poor contact between the nickel sponge and the outer wall of the evaporator, these items being simply close fitting, with no attempt being made to bond them together. Poor contact at this point will reduce the heat transfer to the ammonia in the superheat region without diminishing the undesirable axial conduction.

9.5 DISCUSSION

The considerable scatter apparent on the graphs of both theoretical and experimental results is due mostly to the variation of atmospheric temperature between the different test runs. The runs were spread over a period of four days, each run requiring at least two hours and often more than three hours for steady state conditions to develop.

In estimating the mass flow rate of ammonia, allowance was made in each run for the small quantity of liquid ammonia accumulated in the evaporator and pipework. Additional factors affecting the estimated flow rate would be temperature and pressure at the outlet orifice. At the start of a run, the lack of accumulated liquid in the evaporator presented little resistance to the sudden pressure rise when the solenoid valve was opened. As a result, the pressure tended to cycle between about 11 and 30 lb/in^2 initially, with an average of 20 lb/in^2, say, gradually settling down to a much smaller variation after a certain time. This factor would increase the initial flow rate above the steady state value. On the other hand, the higher temperature prevailing at the orifice at the start of a run would reduce the initial flow rate compared with the steady state value. The latter two effects would be of similar magnitude and were assumed to cancel when estimating the true steady state flow rate.

It is of interest that the variation of mean pressure described above illustrates the need for a pressure regulator in the thruster supply line when considering a real thruster system.

The poor heat transfer obtained in the superheat region can not easily be remedied in practice. Brazing of the nickel sponge to the outer wall is not practical because of the adverse action of the ammonia on any copper based metal. Bonding with a high duty adhesive may be possible and some such measure would seem to be essential if the full benefit is to be obtained from the use of the nickel sponge. Without good thermal contact, the sponge could probably be ignored and convective heat transfer could be considered as the means of heating the ammonia. It would be of interest to carry out an additional analysis of the superheat region assuming convective heat transfer and to compare the theory with the experimental results already obtained.

The measurement of boiling region length was hampered by the unduly high temperatures indicated by three of the internal thermocouples. It is assumed that these thermocouples were touching the outer wall which would be warmer than the adjacent sponge. To prevent this effect in future work, the sponge should be drilled before sealing in the evaporator, any run-out of the holes against the outer wall being corrected. In addition, if the thermal contact in the region were improved as described in the previous paragraph, the recorded temperature errors should be negligible.

More realistic evaporator performance would be obtained in future work if the wall thickness were considerably reduced. Ease of construction dictated the great thickness employed, at the expense of exaggerated axial conduction heat flow which reduced the superheating power of the evaporator to a very low level.

10. CONCLUSION

A method of analysing the steady state thermal behaviour of metal sponge filled cylindrical evaporators has been derived.

For the particular case study considered, it has been shown that the lowest possible weight would result from the smallest possible diameter (and greatest length) of evaporator. However the requirements of plenum volume and ease of installation in the actual spacecraft make a larger diameter desirable, and the choice of evaporator shape would depend on the detailed system requirements. It has also been shown that mounting flanges should run in a radial rather than an axial direction.

No clear advantage was found for either the simple or double walled type of evaporator. The double walled type naturally exerts much greater control over liquid accumulation and tends to be shorter but heavier, and is, of course, slightly more complex in construction. The choice of type also will depend on the particular requirements of the application, though other applications than the one examined may reveal a more marked superiority of one type or the other. Each application must be considered individually.

The experimental results obtained for the double walled evaporator suggest that the theory would be more realistic if the equivalent sphere derived in section 5.4 were based on the area of the evaporator boiling region rather than the entire evaporator area. The results also reveal the limitations of the experimental rig and indicate the need for bonding of the nickel sponge material to the outer wall.

APPENDIX I

STEADY STATE RADIAL TEMPERATURE DISTRIBUTION IN THE SUPERHEAT REGION

As explained in section 3.3 (b) and depicted in Fig. 17 (b), the radial temperature distribution is expected to be somewhat complex in the superheat region.

Two simplifying assumptions will be made to assist in analyzing the situation :

a) the density of the ammonia vapour and the velocity of flow are constant across the evaporator section ;

b) the rate of change of temperature with axial distance is constant across the evaporator section, i.e. $\frac{\partial T}{\partial x}$ is constant across the section.

It then follows that for an axial element of the evaporator, the total radial flow of heat at any radius must be proportional to the quantity of fluid contained within that radius by the element.

Hence, in the radial region $0 < r < r_E$ the radial variation of temperature is given by the expression

$$k_F \cdot 2\pi r \cdot \Delta x \cdot \frac{\partial T}{\partial r} = K \left(\pi r^2 \cdot \Delta x \right)$$

where K is a constant of proportionality

or

$$\frac{\partial T}{\partial r} = K_1 \cdot r$$

and hence

$$T = K_1 \cdot \frac{r^2}{2} + K_2$$

where K_1 and K_2 are arbitrary constants

then, when $r = r_E$

$$\left(\frac{\partial T}{\partial r} \right)_{r_E} = K_1 \cdot r_E$$

For the spacecraft, i.e. the radial region $r_E < r < r_{SC}$, the radial distribution is given by the following expression derived from equation (16a) by writting $r_{SPH} = r_E$

$$\frac{\partial T_{SC}}{\partial r} = \frac{\Delta T_{SC} \cdot r_E \cdot r_{SC}}{r_{SC} - r_E} \cdot \frac{1}{r^2}$$

Therefore, when $r = r_E$

$$\left(\frac{\partial T_{SC}}{\partial r} \right)_{r_E} = \frac{\Delta T_{SC} \cdot r_{SC}}{\left(r_{SC} - r_E \right) \cdot r_E}$$

But the radial flow of heat at station $r = r_E$ must be constant as given by the two equations above. Therefore one can write

$$k_F \cdot \text{area} \cdot K_1 \, r_E = \frac{k_{SC} \cdot \text{area} \cdot \Delta T_{SC} \cdot r_{SC}}{\left(r_{SC} - r_E \right) \cdot r_E}$$

Hence

$$K_1 = \frac{k_{SC}}{k_F} \cdot \Delta T_{SC} \cdot \frac{r_{SC}}{\left(r_{SC} - r_E \right)} \cdot \frac{1}{r^2}$$

Then, the mean temperature of the evaporator cross-section is given by

$$T_v = \frac{1}{\pi r^2} \int_0^{r_E} T \cdot 2\pi r \cdot dr$$

where

$$T = K_1 \cdot \frac{r^2}{2} + K_2$$

which reduces to

$$T_v = K_1 \cdot \frac{r_E^{\;2}}{4} + K_2$$

Then the value of ΔT_v, as shown in Fig. 17 (b), is given by

$$\Delta T_v = \left(K_1 \cdot \frac{r_E^{\;2}}{2} + K_2\right) - \left(K_1 \cdot \frac{r_E^{\;2}}{4} + K_2\right)$$

$$= \frac{k_{SC}}{k_F} \cdot \frac{\Delta T_{SC}}{4} \qquad \text{if } r_{SC} \gg r_E$$

But

$$\Delta T_{SC} + \Delta T_v = \Delta T$$

or

$$\Delta T_{SC} + \frac{k_{SC}}{4k_F} \cdot \Delta T_{SC} = \Delta T$$

Hence

$$\Delta T_{SC} = \frac{4k_F}{4k_F + k_{SC}} \cdot \Delta T$$

or

$$\frac{T_{AMB} - T_w}{T_{AMB} - T_v} = \frac{4k_F}{4k_F + k_{SC}}$$

APPENDIX II

CONSIDERATION OF TRANSIENT CONDITIONS

Transient conditions may be of interest to the designer if the thruster system application is such that only intermittent operation is required and steady state conditions are never reached in the evaporator. In such a case, the thermal capacity of the evaporator and its surroundings may supply much of the required heat and a smaller evaporator may therefore suffice.

In even the simplest problems, the analysis of transient conduction in three dimensions is not straightforward and for such a complex situation as that of the evaporator and spacecraft, an accurate solution is almost impossible except experimentally. Although an accurate solution is beyond the intended scope of the present study, an approximate approach may be of interest.

(a) Thermal Capacity of the System

A rough estimate of the time to approach steady state conditions can be obtained by considering the thermal capacity of the evaporator and spacecraft. A means of computing the steady state conditions has been given in the bulk of this report and the required capacity is simply the difference between the heat content of the system at ambient temperature and during steady state operation.

The thermal capacity of the evaporator is given by

$$Q_E = Q_B + Q_S$$

where

Q_B = thermal capacity of boiling region

Q_S = thermal capacity of superheat region

If W_E = weight of evaporator, we can write

$$Q_E = W_E \cdot Cp_E \cdot \frac{\lambda_B}{\lambda_T} \left(T_{AMB} - T_L\right) + \int_0^{\lambda_s} \frac{W_E \cdot Cp_E}{\lambda_T} \left(T_{AMB} - T_v\right) dx$$

which reduces to

$$Q_E = \frac{W_E \cdot Cp_E \cdot \Delta T_0}{\lambda_T} \left\{ \lambda_B + \left[\frac{1}{c_6} \left(e^{c_6 \lambda_s} - 1 \right) + \frac{c_6}{c_7{}^2} \left(\frac{1}{e^{c_{10} \lambda_s}} - e^{c_6 \lambda_s} \right) \right] \right\}$$

or

$$Q_E = W_E \cdot Cp_E \cdot \Delta T_0 \quad \frac{\left(\lambda_B - \frac{1}{c_6}\right)}{\lambda_T}$$

unless λ_s is extremely small.

The thermal capacity of the spacecraft can be calculated as follows. For concentric homogeneous spheres, we obtained equation (16) describing the radial variation of temperature i.e.

$$T_{SC} = T_{AMB} + \left(\frac{T_{AMB} - T_w}{r_{SC} - r_{SPH}} \right) \cdot r_{SPH} \cdot \left(1 - \frac{r_{SC}}{r} \right)$$

If $r_{SC} \gg r_{SPH}$, one can write

$$T_{SC} = T_{AMB} + \left(T_{AMB} - T_w \right) \cdot \frac{r_{SPH}}{r_{SC}} \cdot \left(1 - \frac{r_{SC}}{r} \right)$$

For a cylindrical evaporator, we obtained equation (18) i.e.

$$r_{SPH} = r_E \sqrt{0.5 + \frac{\lambda_T}{d}}$$

An overall expression for $(T_{AMB} - T_w)$ averaged over the entire sphere, is required. It is logical to use the same factor as appears in the expression for Q_E above.

i.e.

$$(T_{AMB} - T_w) = \frac{\Delta T_0 \left(\lambda_B - \frac{1}{c_6}\right)}{\lambda_T}$$

One can now write

$$T_{SC} = T_{AMB} + \Delta T_0 \cdot \frac{\left(\lambda_B - \frac{1}{c_6}\right)}{\lambda_T} \cdot \frac{r_E}{r_{SC}} \cdot \sqrt{0.5 + \frac{\lambda_T}{d}} \cdot \left(1 - \frac{r_{SC}}{r}\right)$$

The thermal capacity of the spacecraft is then obtained by considering elemental spherical shells of thickness dr

$$Q_{SC} = \int_{r_{SPH}}^{r_{SC}} Cp_{SC} \cdot \rho_{SC} \cdot 4\pi r^2 \left(T_{AMB} - T_{SC}\right) dr$$

which reduces to

$$Q_{SC} = 2\pi \, Cp_{SC} \cdot \rho_{SC} \cdot \Delta T_0 \sqrt{0.5 + \frac{\lambda_T}{d}} \cdot \frac{\left(\lambda_B - \frac{1}{c_6}\right)}{3\,\lambda_T} \cdot r_E \cdot r_{SC}^{\,2}$$

when $r_{SC} \gg r_{SPH}$

(b) Saturation Time of the System

Let θ be defined as the saturation time of the thermal sink formed by the evaporator and spacecraft. The heat which must be supplied to the ammonia in time θ in order to evaporate and superheat to the required level is given by

$$Q_{TOTAL} = m \left[\Delta H_B + Cp_v \left(T_{ULT} - T_L \right) \right] \cdot \theta$$

Q_{TOTAL} can be equated to the sum of Q_E and Q_{SC} to obtain the value of θ.

We will perform a sample calculation, using parameter values corresponding to the double walled evaporator with five cubic inch volume described in section 8.3. It will be remembered that in addition to the parameters specified in sections 7.1 and 8.2, the following values were established :

$$W_E = 0.225 \text{ lb}$$

$$d = 1.055 \text{ in}$$

$$\lambda_T = 6.15 \text{ in}$$

Referring back to the computer programme, one can also obtain

$$\lambda_B = 4.70 \text{ in}$$

$$c_6 = -22.96$$

Values are also required for Cp_E, Cp_{SC}, ρ_{SC}, r_{SC}.

The specific heats of stainless steel and nickel are 0.116 and 0.109 respectively, and since 70-80 percent of the evaporator mass is stainless steel, one can write

$$Cp_E = 0.115 \text{ Btu/lb } ^{0}\text{F}$$

Assuming an aluminium alloy spacecraft structure, the specific heat will be

$$Cp_{SC} = 0.214 \text{ Btu/lb } ^{0}\text{F}$$

The density of the spacecraft structure is the product of the density of aluminium alloy, 168.5 lb/in^2, and the assumed structural density, 1/30 of the solid material. Hence

$$\rho_{SC} = 5.62 \text{ lb/ft}^3$$

It should be pointed out that since transient effects are now being considered, the thermal capacity of the spacecraft equipment and payload may have to be taken into account. However, if we continue to assume poor thermal contact between structure and equipment, the thermal content of the equipment will have little effect on the rate of heat flow to the evaporator. In other words, although the potential heat capacity of the equipment may be considerable, its usefulness will be restricted by the available rate of heat transfer.

The choice of spherical radius for the spacecraft is somewhat arbitrary although the value of θ can be seen to be governed by Q_{SC} which is proportional to the square of r_{SC}. Being careful therefore to choose a realistic figure, let us write

$$r_{SC} = 1.5 \text{ ft}$$

The formulae developed in section (a) of this Appendix can now be applied to obtain

$$Q_E = 9.8 \text{ Btu}$$

$$Q_{SC} = 59.6 \text{ Btu}$$

and

$$Q_{TOTAL} = (0.0551)\,\theta \text{ Btu}$$

Hence

$$\theta = \frac{9.8 + 59.6}{0.0551} = 1{,}258 \text{ seconds}$$

or approximately $\theta = 21$ minutes.

A word of explanation is required concerning the precise meaning of this value for θ. It is the length of time for which the system could operate if the evaporator were drawing heat only from its own thermal energy content and that of the spacecraft, with respect to steady state conditions. In practice of course, the spacecraft continually receives thermal energy from external sources such as the sun, and an increasing amount of heat will be extracted from those sources as time goes by, until steady state is effectively reached. The situation is shown in Fig. 18 which is schematic only and not intended to be scaled.

The extraction of heat from the thermal content of the system would appear to be an exponential function of time but the value of the exponential coefficient is indeterminate by this simple study. One must therefore be content with the given value of θ as a rough guide to the time during which transient effects are significant. For an application where the maximum continuous operating time of the system is less than θ, one can say that transient effects may be worth further investigation, perhaps experimentally, with a view to a possible reduction in the size and weight of evaporator required.

ACKNOWLEDGEMENTS

This Technical Report was prepared during the course of a NASA International University Fellowship at the University of Cincinnati during the period September 1966-August 1967.

The author is indebted to the staff of the Space Power Propulsion Section at the General Electric Company, Evendale, for the opportuny to carry out the study contained in this report and for the loan of experimental equipment.

The author gratefully acknowledges the support of the ESRO and of the National Aeronautics and Space Administration for the duration of these studies at the University of Cincinnati.

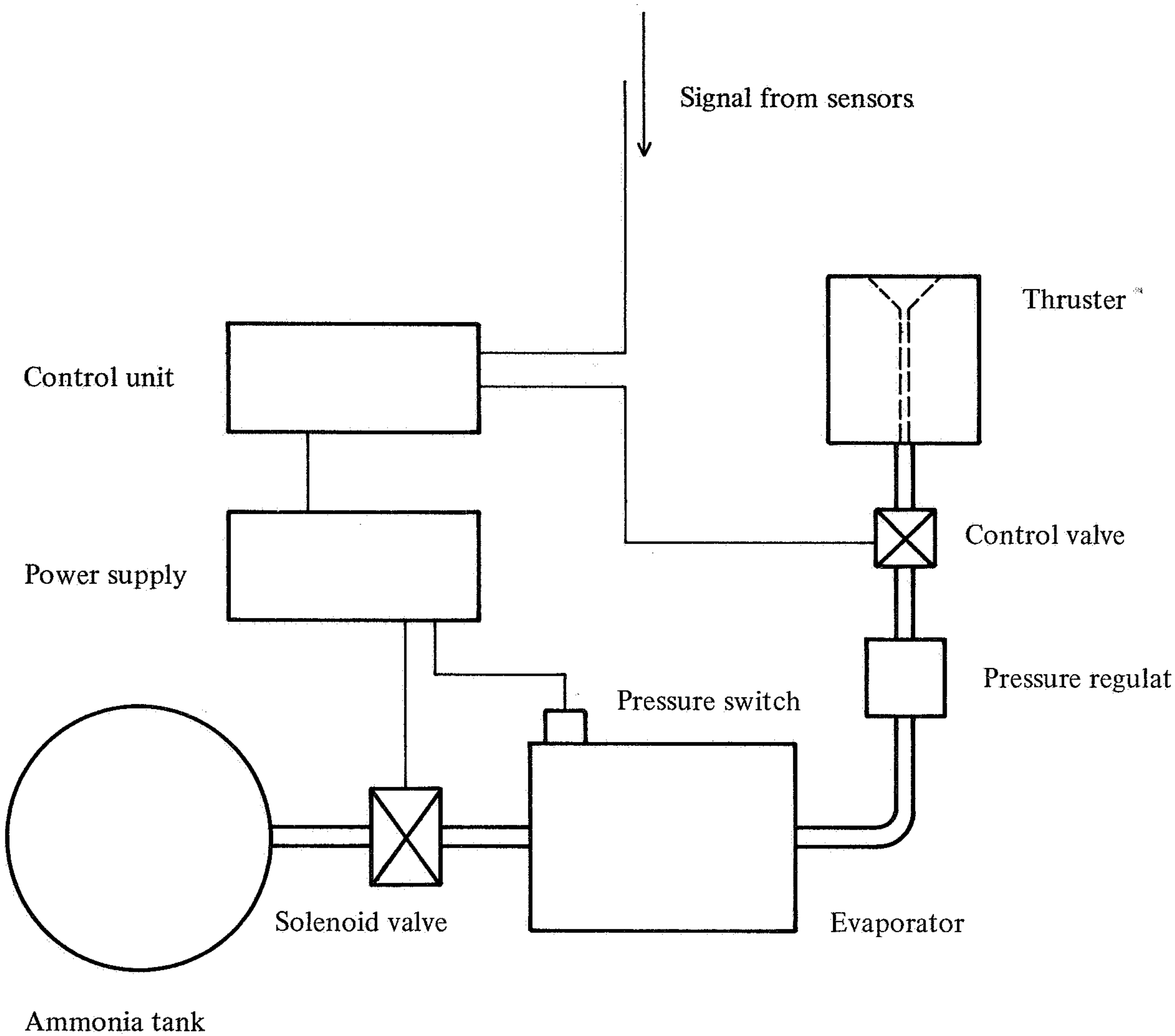

Figure 1.- General layout of typical ammonia thruster system

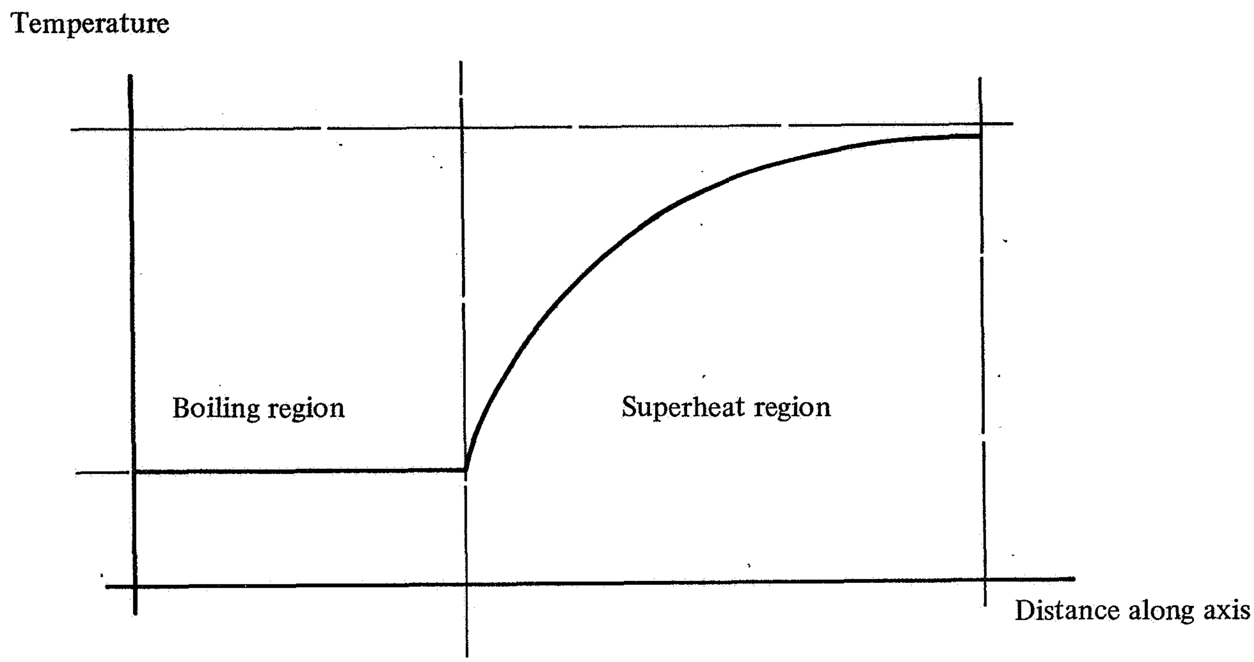

(a) Temperature variation along evaporator axis

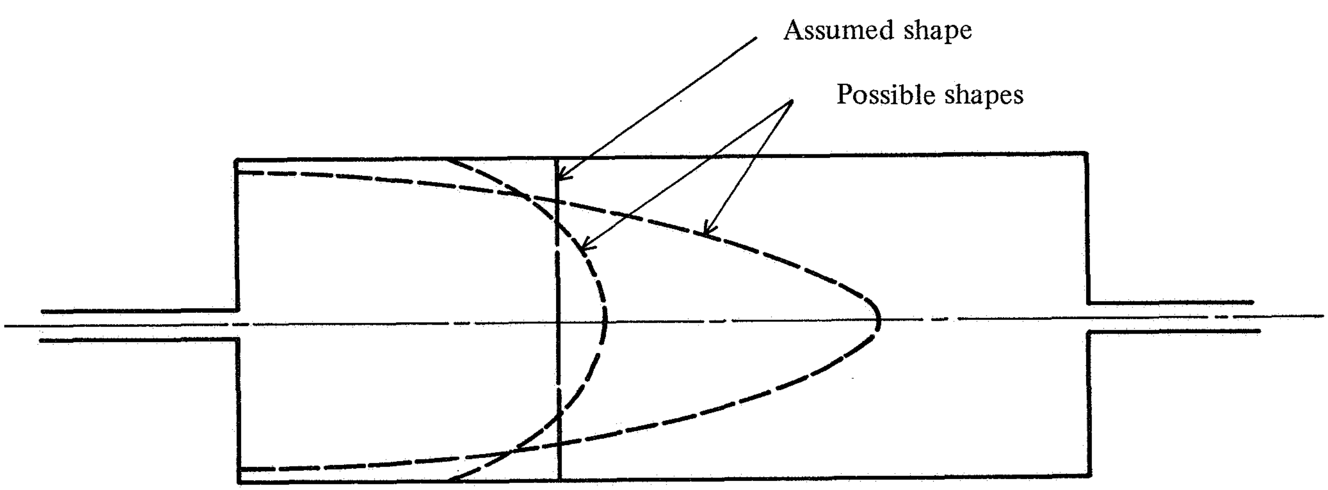

(b) Liquid boundary shape

Figure 2.- Axial distribution of the temperature and shape of the liquid boundary

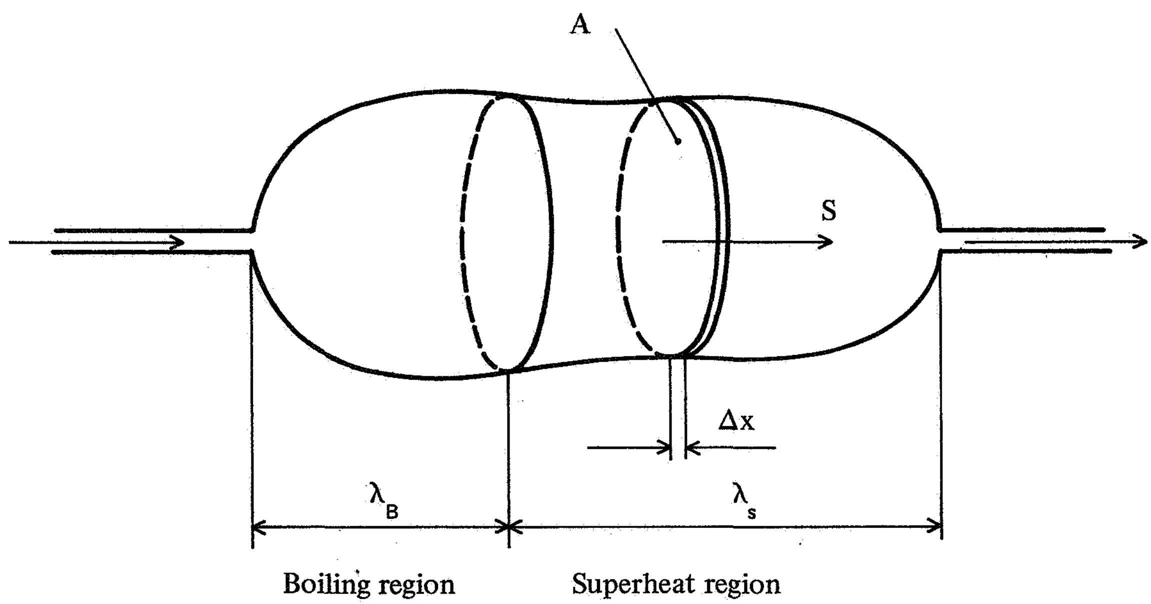

Figure 3.- Evaporator analytical model

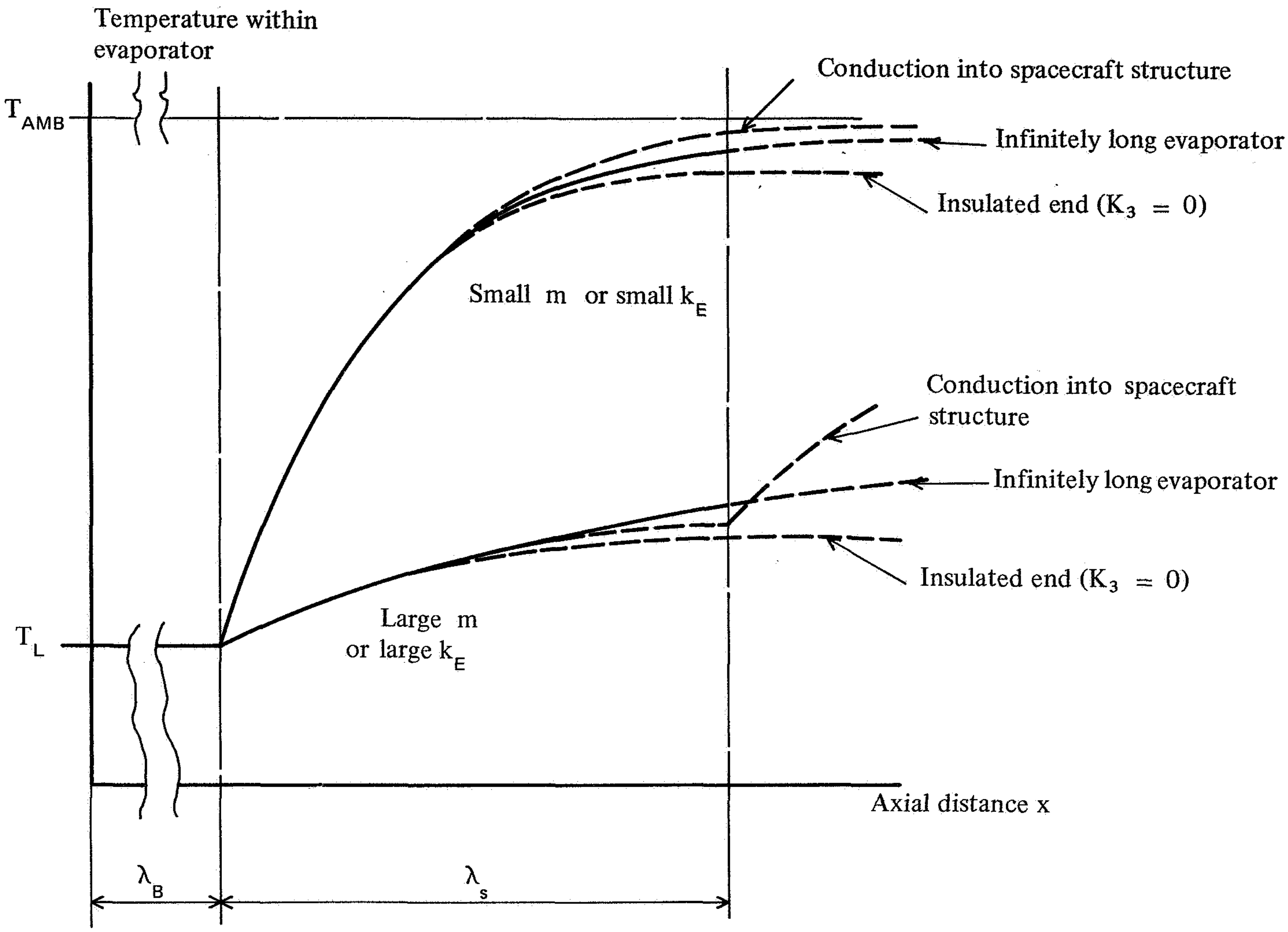

Figure 4.- Detailed temperature variation along the evaporator axis

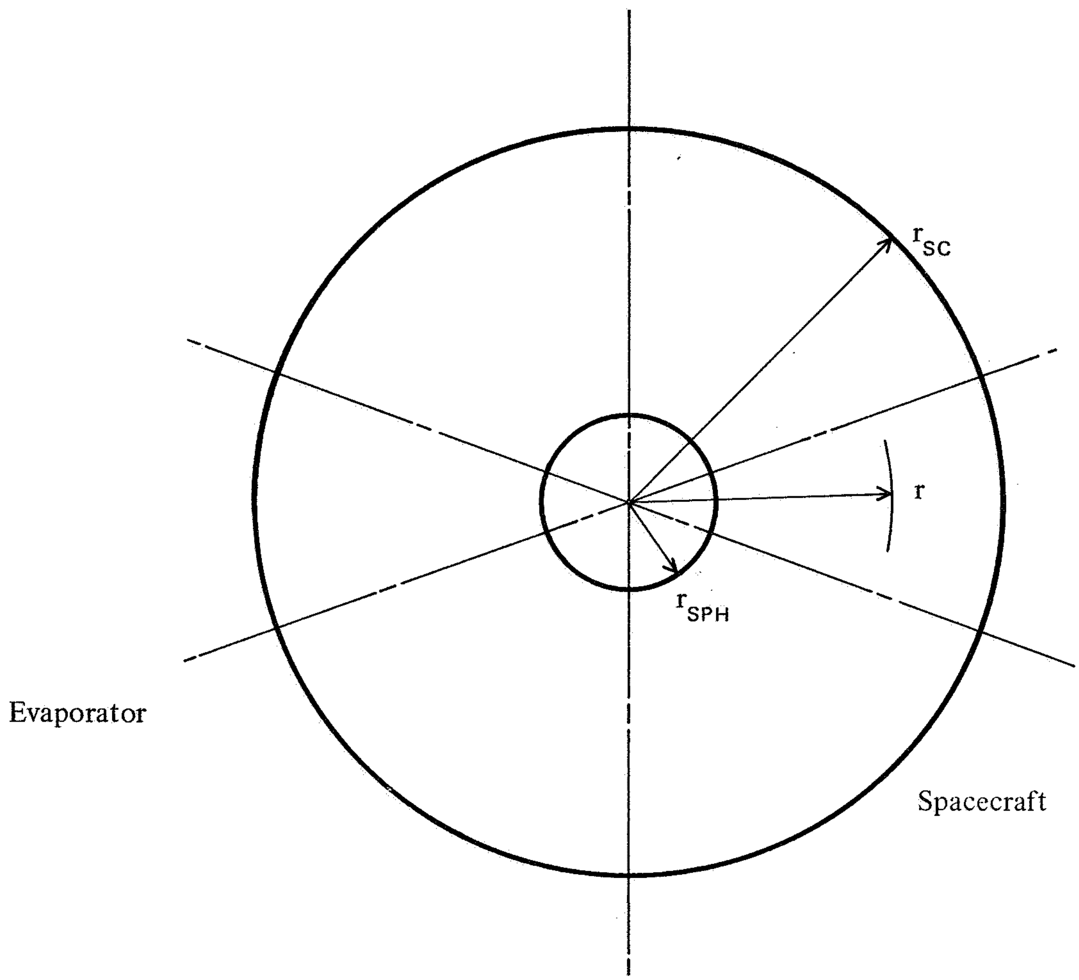

Figure 5.- Idealised spherical model for conductive heat transfer

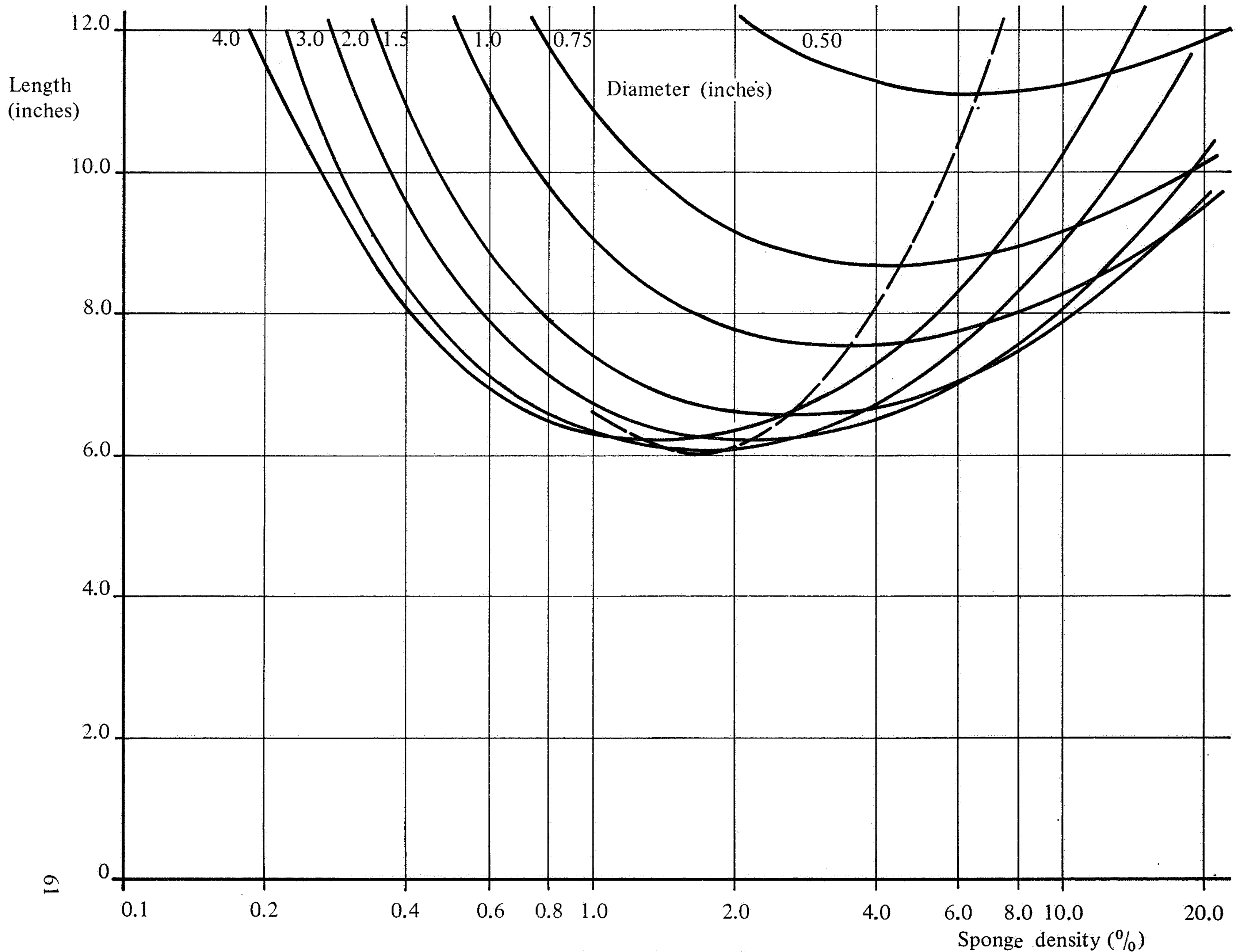

Figure 6.- Length of simple evaporator

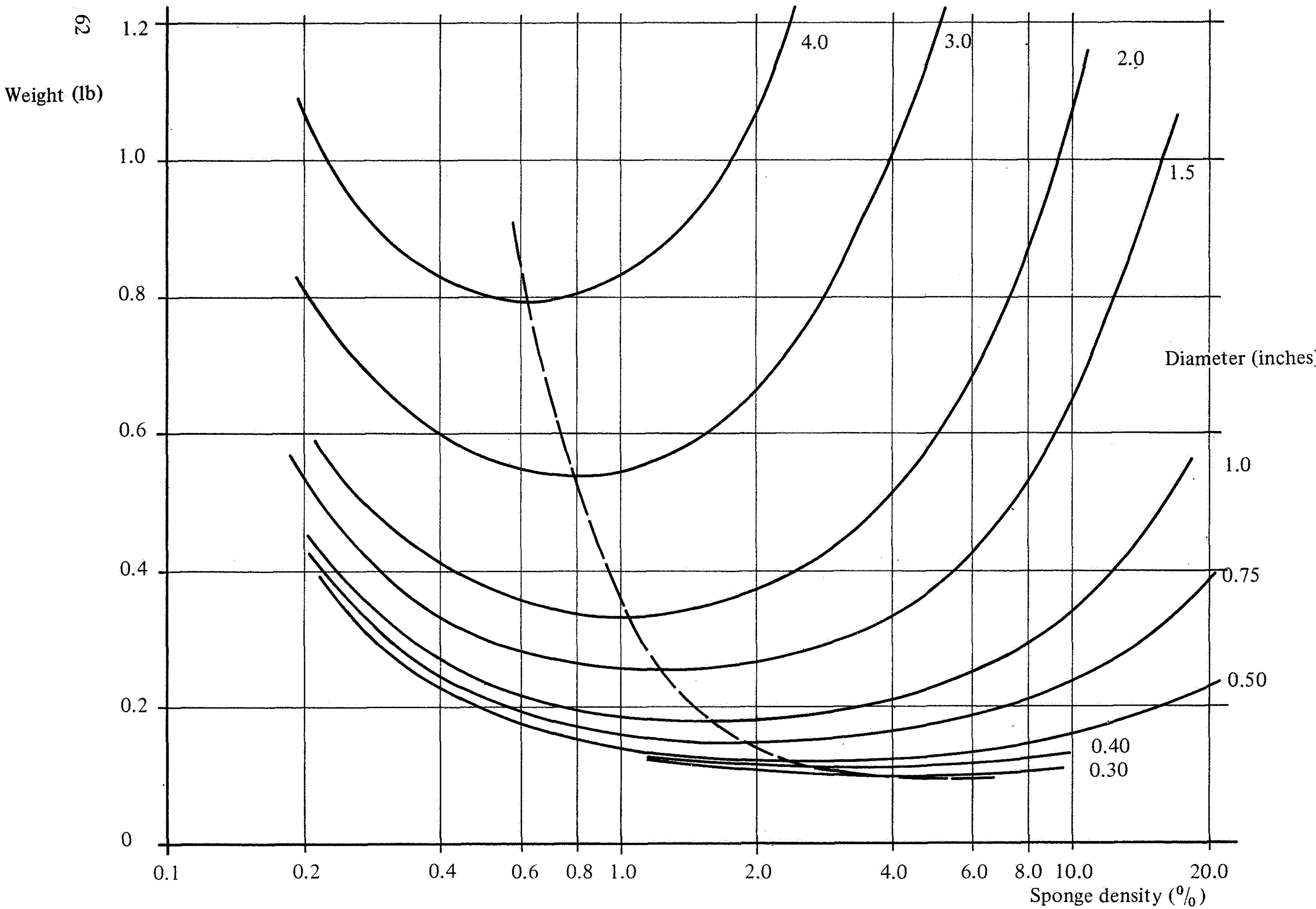

Figure 7.- Weight of simple evaporator

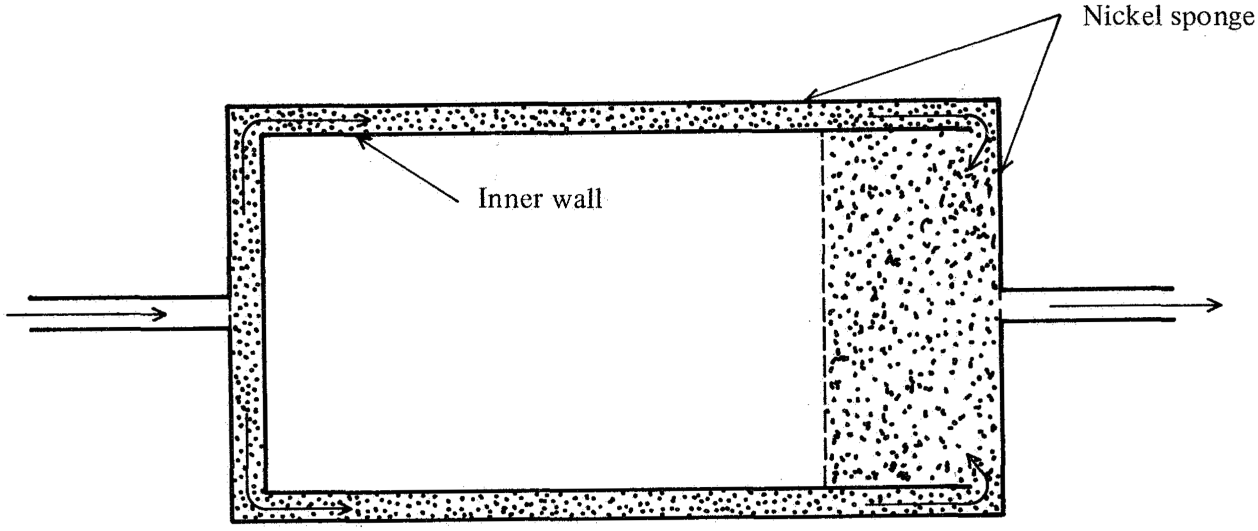

Figure 8.- Section through double-walled evaporator

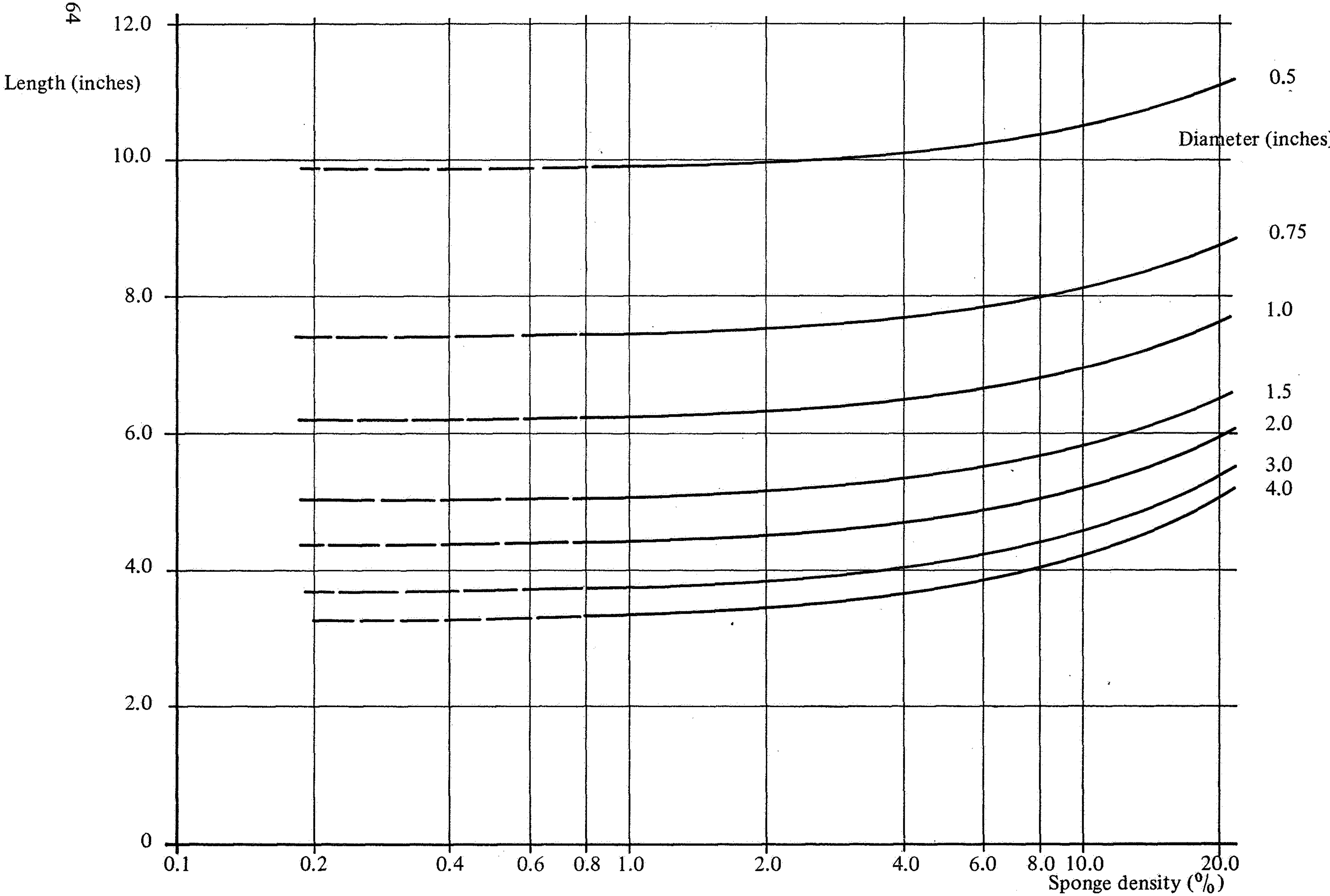
Length (inches)
12.0
10.0
8.0
6.0
4.0
2.0
0
0.1
0.2
0.4
0.6
0.8
1.0
2.0
4.0
6.0
8.0
10.0
20.0
Sponge density (%)
Diameter (inches)
0.5
0.75
1.0
1.5
2.0
3.0
4.0

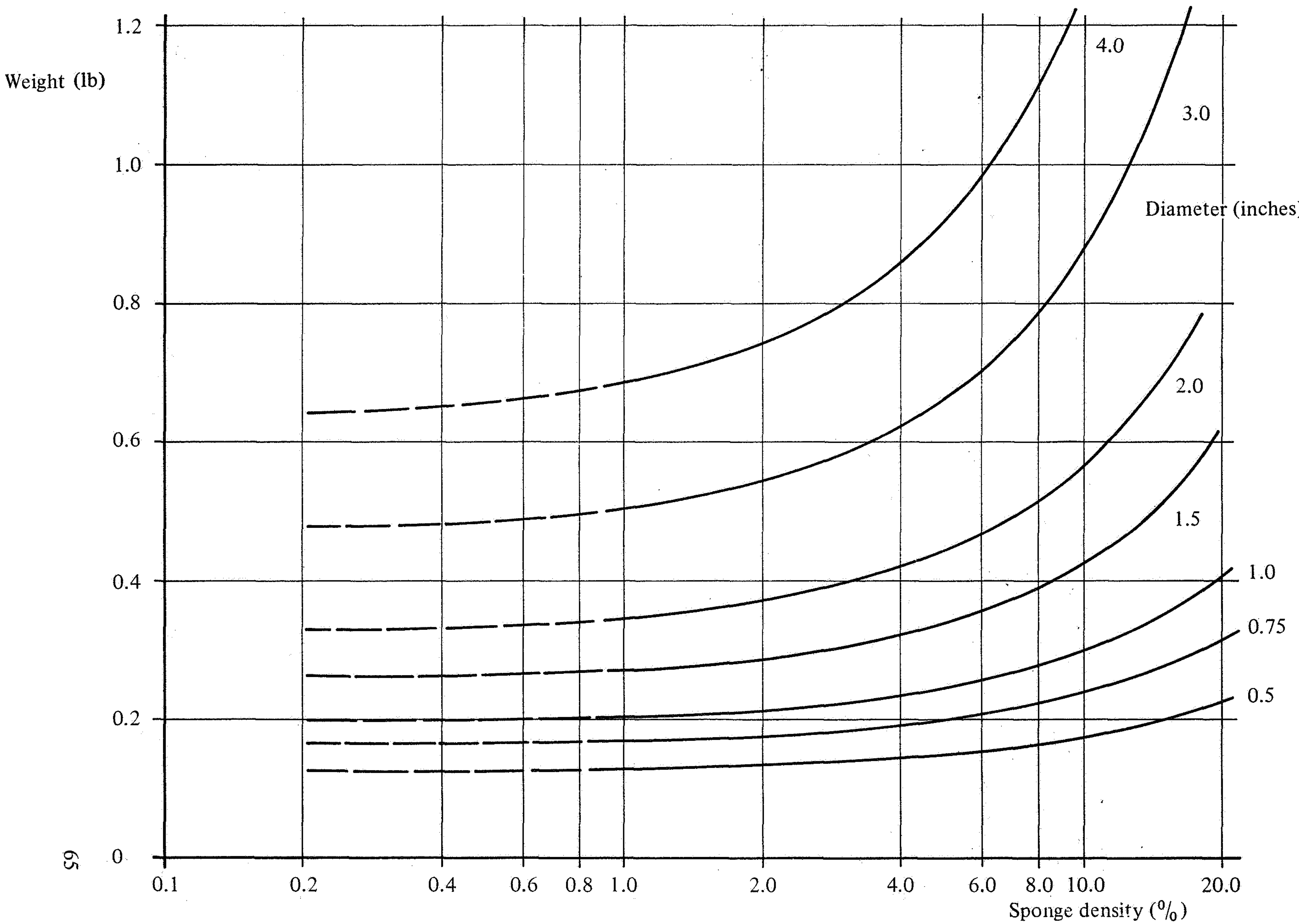

Figure 10.- Weight of double-walled evaporator

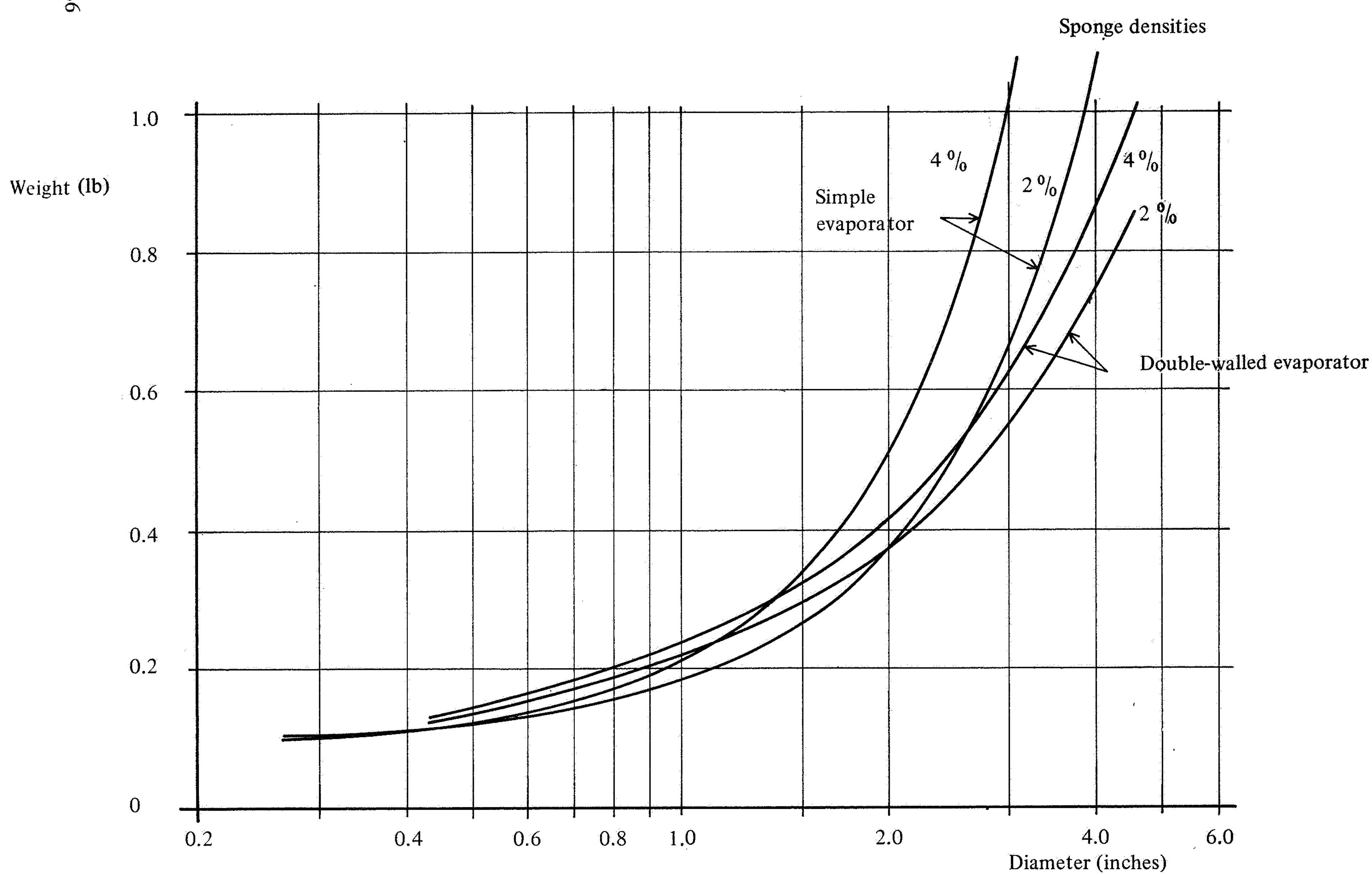

Figure 11.- Weight of simple and double-walled evaporators

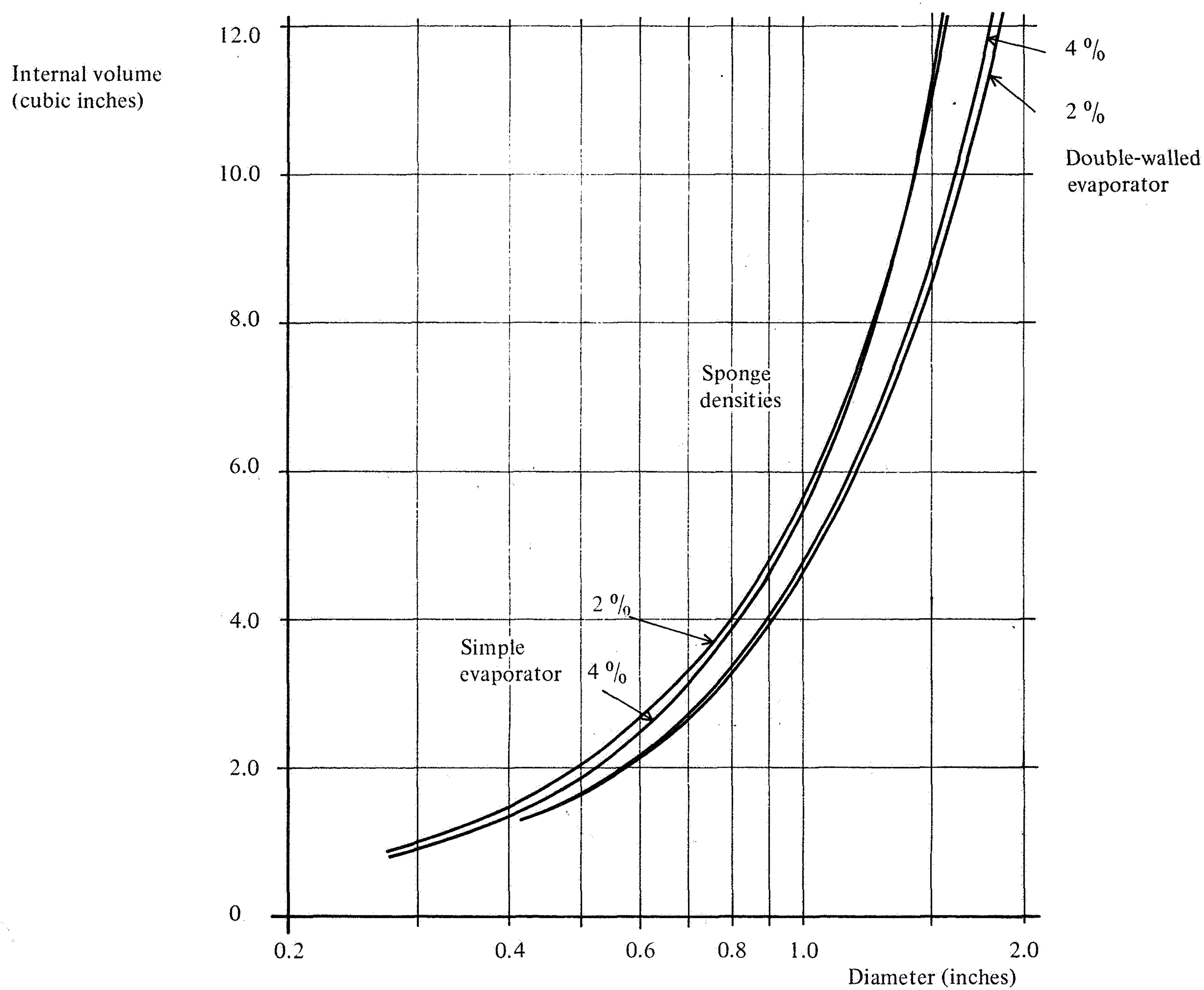

Figure 12.- Internal volume of simple and double-walled evaporators

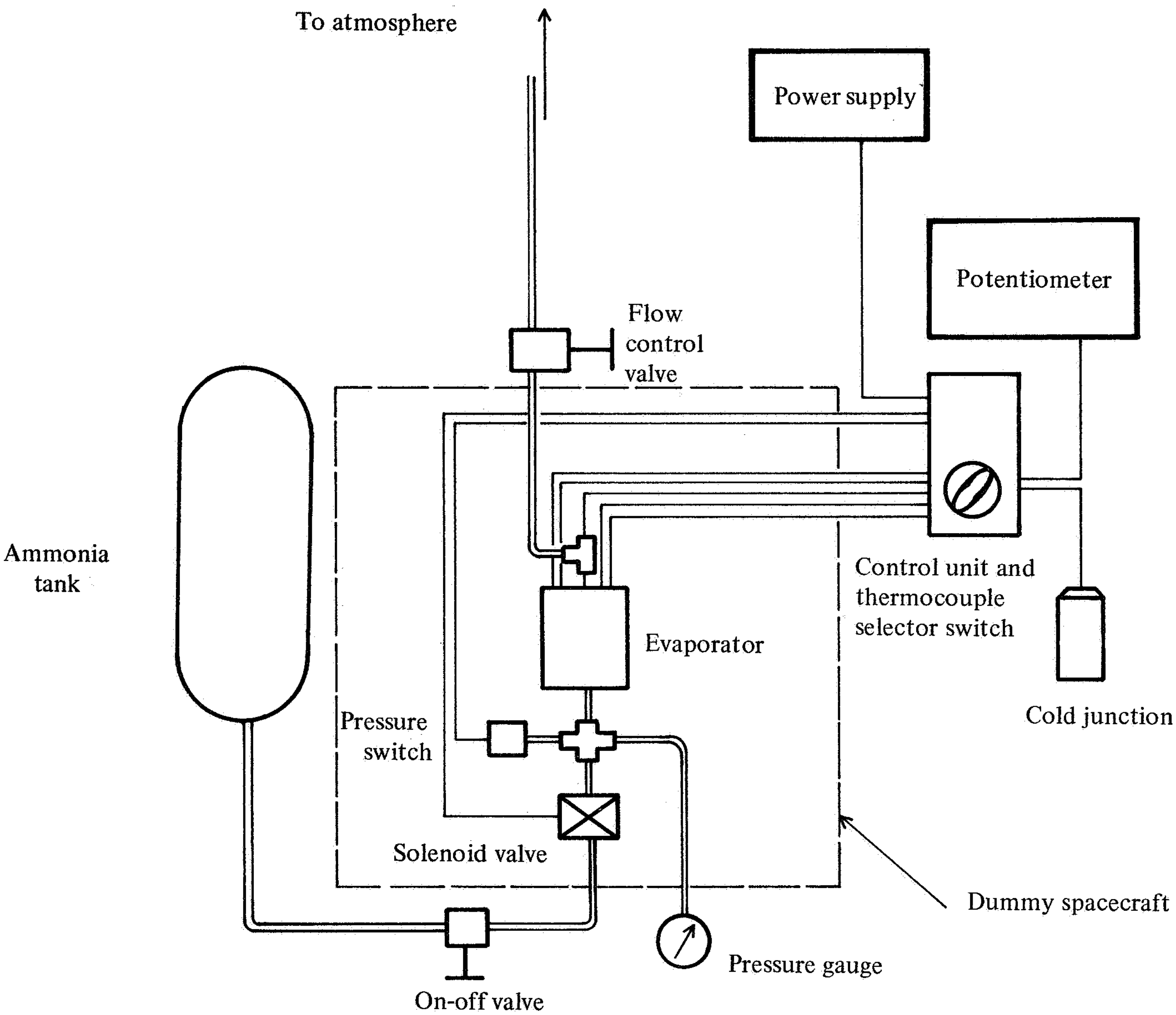

Figure 13.- Experimental system layout

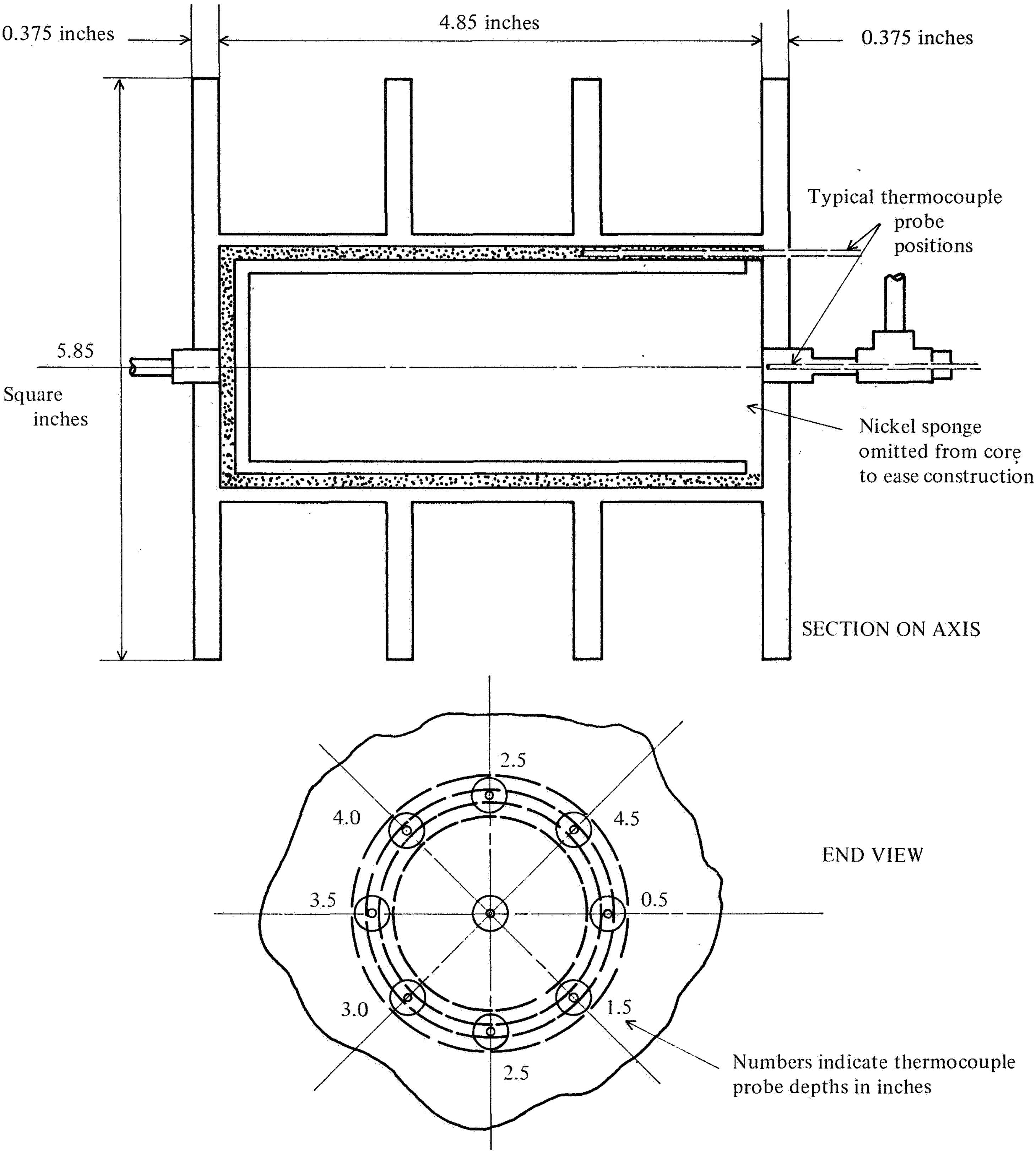

Figure 14.- Details of experimental evaporator and instrumentation

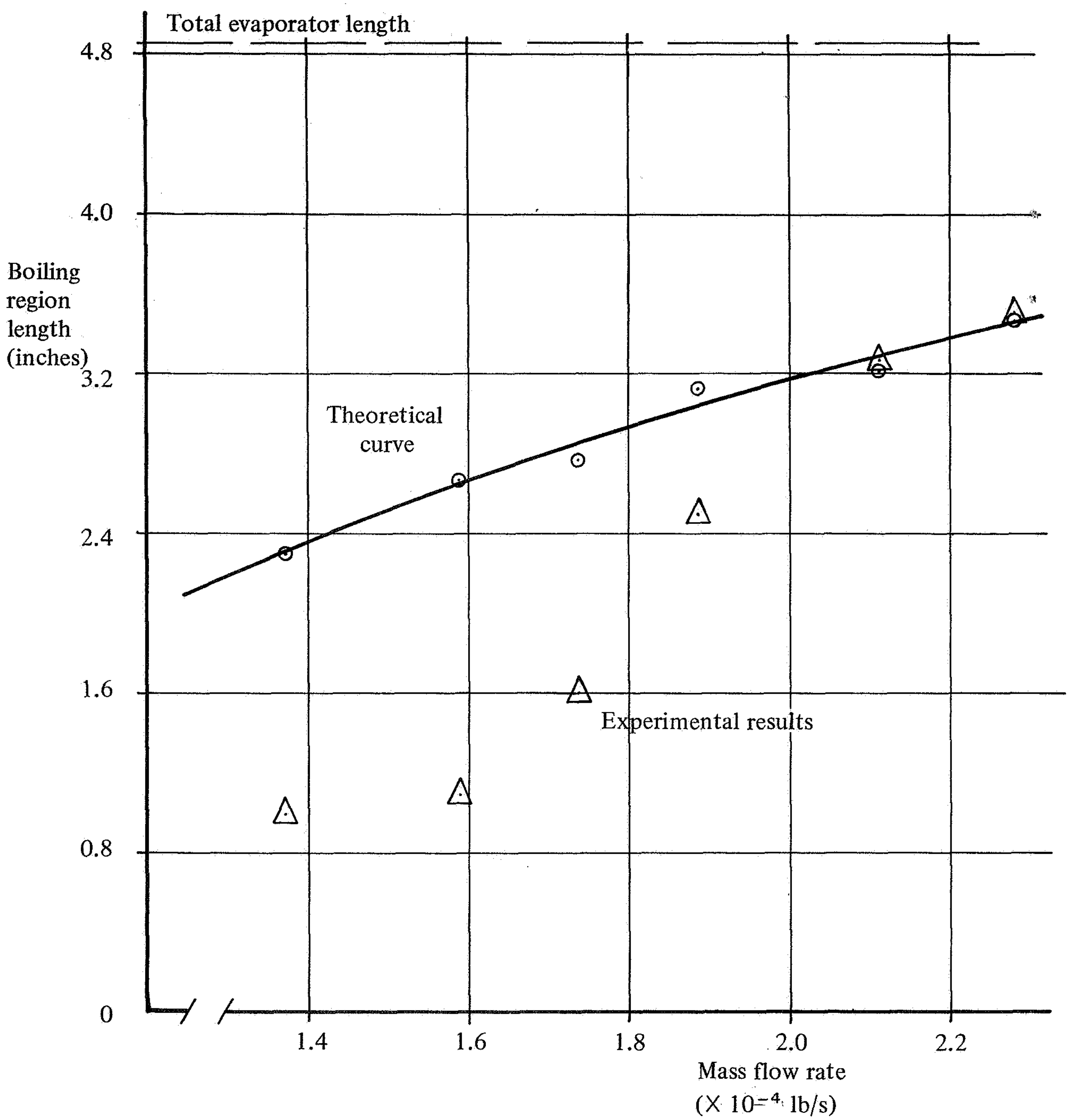

Figure 15.- Comparison of theoretical and experimental variation of boiling region length

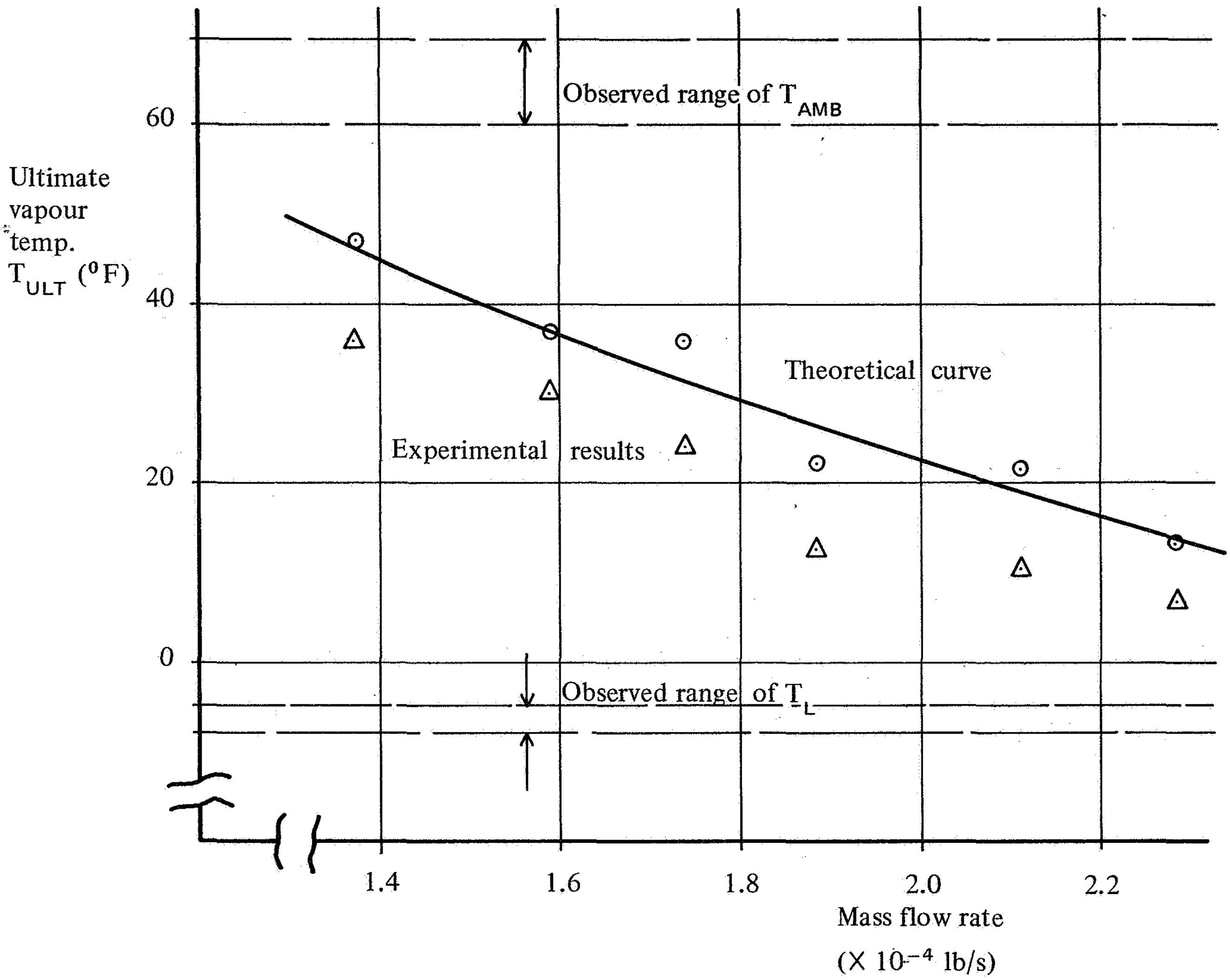

Figure 16.- Comparison of theoretical and experimental variation of ultimate vapour temperature

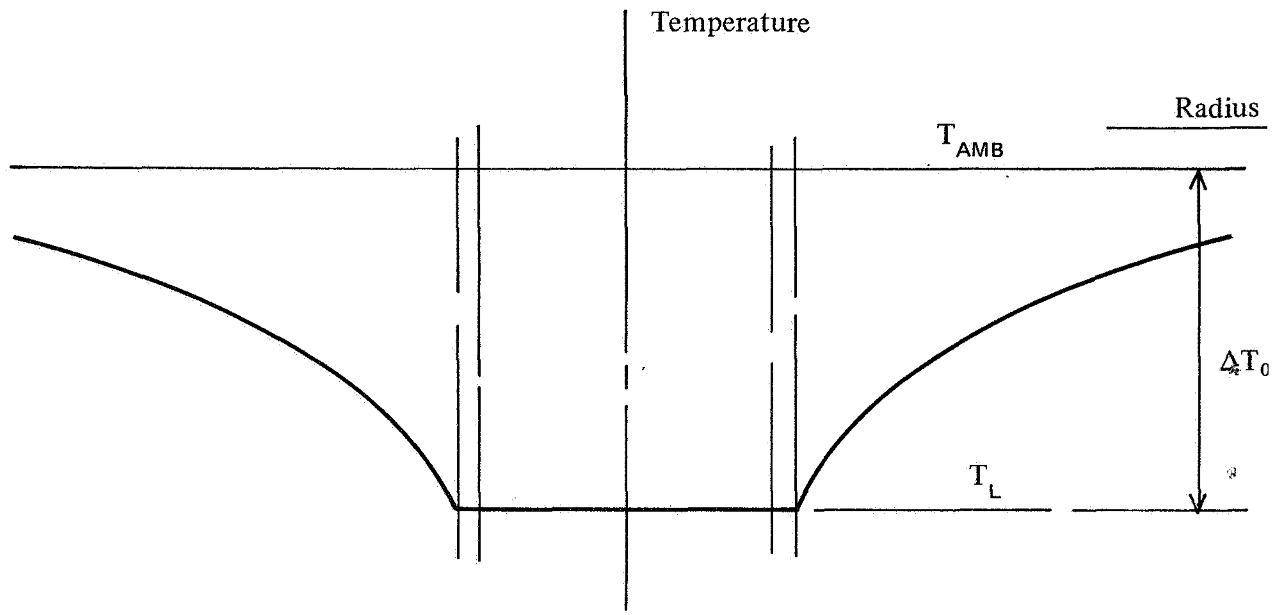

(a) Radial temperature distribution in boiling region

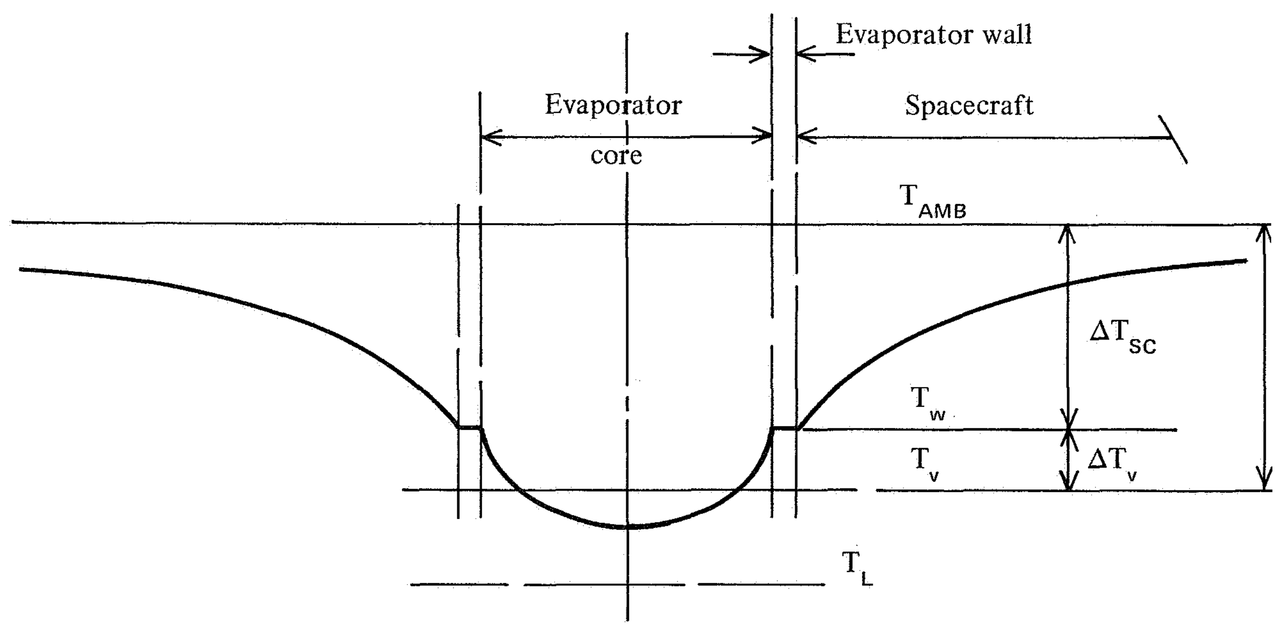

(b) Radial temperature distribution in superheat region of simple evaporator

Figure 17.- Radial distribution of the temperature

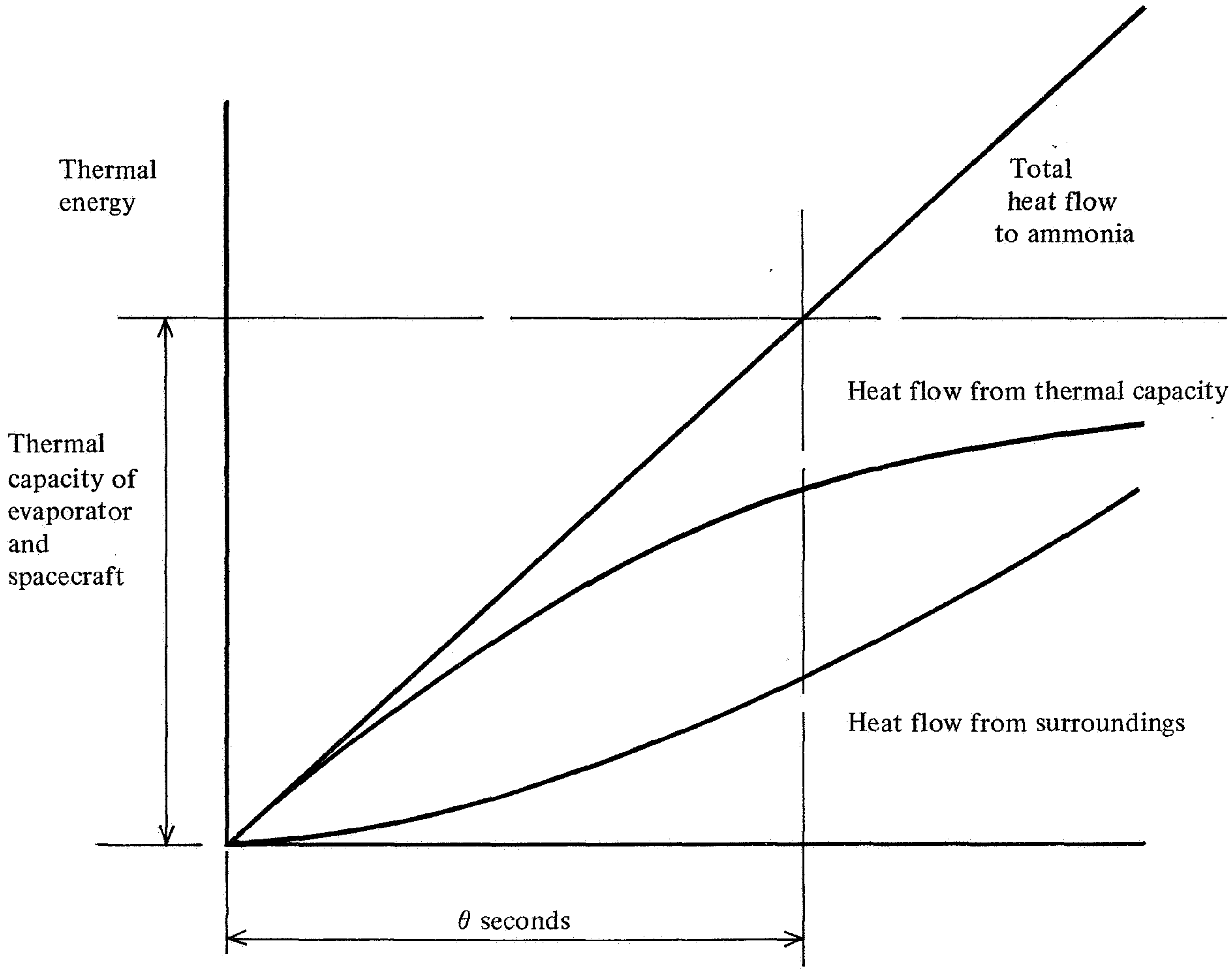

Figure 18.- Transient thermal energy flow

SINED
SYNTHESES - NOTICES - EDITIONS
23 rue de l'Ancienne Mairie
92 - BOULOGNE
Tél. 825.64.81